734 J. Med. Chem. 2011, 54, 734–750
DOI: 10.1021/jm101383f

Journal of Medicinal Chemistry Article

Incorporation of Basic Side Chains into Cryptolepine Scaffold: Structure−Antimalarial Activity Relationships and Mechanistic Studies

João Lavrado,[†] Ghislain G. Cabal,[‡] Miguel Prudêncio,[‡] Maria M. Mota,[‡] Jiri Gut,[§] Philip J. Rosenthal,[§] Cecília Díaz,[∥] Rita C. Guedes,[†] Daniel J. V. A. dos Santos,[†] Elena Bichenkova,[⊥] Kenneth T. Douglas,[⊥] Rui Moreira,*[,†] and Alexandra Paulo[†]

[†]*Research Institute for Medicines and Pharmaceutical Sciences (iMed.UL), Faculty of Pharmacy, University of Lisbon. Av. Prof. Gama Pinto, 1649-003 Lisbon, Portugal,* [‡]*Unidade de Malária, Instituto de Medicina Molecular, Universidade de Lisboa, 1649-028 Lisboa, Portugal,* [§]*Department of Medicine, San Francisco General Hospital, University of California, San Francisco, Box 0811, San Francisco, California 94143, United States,* [∥]*Departamento de Bioquímica, Escuela de Medicina and Instituto Clodomiro Picado, Universidad de Costa Rica, 2060 San José, Costa Rica, and* [⊥]*School of Pharmacy and Pharmaceutical Sciences, University of Manchester, Oxford Road, Manchester M13 9PT, United Kingdom*

Received June 7, 2010

The synthesis of cryptolepine derivatives containing basic side-chains at the C-11 position and their evaluations for antiplasmodial and cytotoxicity properties are reported. Propyl, butyl, and cycloalkyl diamine side chains significantly increased activity against chloroquine-resistant *Plasmodium falciparum* strains while reducing cytotoxicity when compared with the parent compound. Localization studies inside parasite blood stages by fluorescence microscopy showed that these derivatives accumulate inside the nucleus, indicating that the incorporation of a basic side chain is not sufficient enough to promote selective accumulation in the acidic digestive vacuole of the parasite. Most of the compounds within this series showed the ability to bind to a double-stranded DNA duplex as well to monomeric hematin, suggesting that these are possible targets associated with the observed antimalarial activity. Overall, these novel cryptolepine analogues with substantially improved antiplasmodial activity and selectivity index provide a promising starting point for development of potent and highly selective agents against drug-resistant malaria parasites.

Introduction

The emergence and spread of chloroquine-resistant *Plasmodium falciparum* parasites has been a major global health problem and contributes significantly to the continued high prevalence of malaria.[1,2] New, safe, and effective drugs active against multidrug resistant *P. falciparum* strains are thus urgently needed.[1,3] Medicinal plants have long been used for treating parasitic diseases, including malaria, and constitute an important source of new molecules for lead optimization programs, as exemplified by the success of artemisinin and its derivatives.[4−8]

Cryptolepine, **1** (Figure 1), is an indolo[3,2-*b*]quinoline alkaloid first isolated in 1929[9] from the roots of *Cryptolepis sanguinolenta*, a shrub used in traditional medicine for the treatment of malaria in Central and West Africa. In addition, cryptolepine also exerts antibacterial, antifungal, antihyperglycemic, anti-inflammatory, and antitumor activities.[10,11] Cryptolepine displays potent antiplasmodial activity against both chloroquine-resistant and sensitive strains but unfortunately also presents cross-resistance with chloroquine. Moreover, the cytotoxic properties of this alkaloid, which are likely to result from intercalation of **1** into DNA GC-rich sequences and inhibition of topoisomerase II,[12−14] preclude its clinical use.[14−16]

The antimalarial mechanism of action of cryptolepine is not yet clarified, but it was shown that this activity is due, at least in part, to a chloroquine-like action, i.e. inhibition of hemozoin (malaria pigment) formation.[17−20] Degradation of hemoglobin by malaria parasite proteases releases ferriprotoporphyrin IX (FPIX), which is detoxified by crystallization to hemozoin in the acidic digestive vacuole of the parasite. Chloroquine (CQ[a]), **2** (Figure 1), and related 4-aminoquinoline antimalarials bind to FPIX via $\pi-\pi$ stacking interaction of the quinoline moiety with the porphyrin ring, thus inhibiting detoxification.[21] It has been proposed that chloroquine can also bind as a capping molecule to hemozoin crystals, inhibiting crystal growth with consequent accumulation of toxic free heme in the digestive vacuole of the parasite.[22] However, a cellular localization study by Arzel and co-workers showed that cryptolepine accumulates into specific structures of the parasite that could correspond to the parasite nucleus.[23] The data provided by Arzel and co-workers suggest that the affinity of **1** for heme may not be sufficient to drive its accumulation in the digestive vacuole in the absence of a pH-dependent trapping mechanism, and indirectly point toward additional (or alternative) mechanisms of action for cryptolepine other than via hemozoin binding in the digestive vacuole. Interaction of cryptolepine with parasite DNA might be considered as an alternative mechanism contributing to the antiprotozoal activity of cryptolepine analogues.[23]

*To whom correspondence should be addressed: Phone: +351 217 946 477. Fax: +351 217 946 470. E-mail: rmoreira@ff.ul.pt.

[a] Abbreviations: HUVEC, human umbilical vein endothelial cells; PPA, polyphosphoric acid; CQ, chloroquine; SI, selectivity index; RI, resistance index; GFP, green fluorescent protein; FP, falcipain.

 Published on Web 01/05/2011

Recently, on the basis of the observation that a basic amino side chain is a major requirement for chloroquine accumulation in the acid digestive vacuole of the parasite, we synthesized a small series of cryptolepine analogues containing diaminoalkane side chains (−NH-linker-NR^1R^2) at C-11. These compounds were very potent against the *P. falciparum* W2 chloroquine-resistant strain, with IC_{50} values ranging from 22 to 184 nM.[24] From a preliminary cytotoxicity study using human umbilical vein endothelial cells (HUVEC), several compounds emerged with selectivity ratios that were improved compared to **1**. This promising result prompted us to investigate structure−activity relationships (SAR) to decipher the structural requirements of side-chains at C-11 of the cryptolepine scaffold, i.e. analogues **3a**−**y** (Figure 1), for improved antiplasmodial activity and selectivity relative to the lead compound. The diversity of the side chain was explored by varying the nature and length of the linker between the two nitrogen atoms as well as the substitution pattern and basicity of the distal amino group. Antiplasmodial and cytotoxic activities of cryptolepine derivatives **3a**−**y** were evaluated against different *P. falciparum* strains and a mammalian cell line. Taking advantage of the fluorescence properties of the indoloquinoline nucleus, fluorescence microscopy was used to evaluate the subcellular localization of the compounds in parasites. To identify possible biological targets, which could potentially be linked to the antiplasmodial activity of cryptolepine derivatives, additional experiments were performed to determine the ability of cryptolepine analogues to interact with hematin, with cysteine proteases involved in the degradation of host hemoglobin (falcipain-2 and -3) and with DNA oligonucleotide duplex.

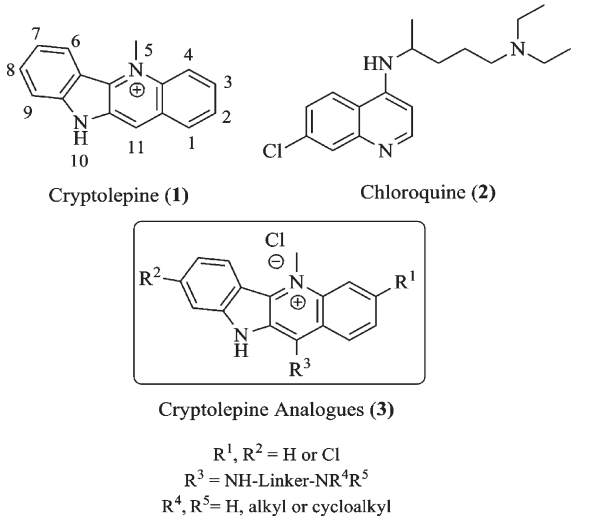

Figure 1. Structures of cryptolepine (**1**), chloroquine (**2**), and cryptolepine analogues (**3a**−**y**).

Chemistry

Cryptolepine analogues **3a**−**y** were synthesized according to the route depicted in Scheme 1, via the 11-Cl intermediates **10**, based on the procedure developed by Görlitzer and Weber[25,26] and adapted by Bierer.[27,28] Anthranilic acids, **4**, were treated with bromoacetyl bromide to afford the corresponding bromoacetyl derivatives **5**, which were then reacted with the appropriate aniline to give compounds **6**. Acid-catalyzed cyclization of **6** with polyphosphoric acid (PPA) gave the indolo[3,2-*b*]quinolin-11-ones (quindolones) **7**, which, by reaction with $POCl_3$, gave the corresponding substituted 11-chloro-indolo[3,2-*b*]quinolines (11-chloroquindolines) **8**. Hydrogenation of **8a** with 10% Pd−C at 60 psi provided the indolo[3,2-*b*]quinoline (quindoline) **9**. *N*-5 Methylation of **8** and **9** was achieved by reaction with methyl triflate, and the 5-methyl-indolo[3,2-*b*]quinoline derivatives of **8** were then treated with hydrochloric acid to afford the corresponding cryptolepine chlorides, **10**. Finally, cryptolepine derivatives **3a**−**n** and **3r**−**y** were obtained in 30−82% yield by aromatic nucleophilic substitution on **10** with excess of appropriate amine. Compounds **3o**−**q** were synthesized by reaction of **3n** with isobutyraldehyde, benzylaldehyde, and salicylaldehyde

Scheme 1. Synthesis of Cryptolepine (**1**) and Cryptolepine Analogues **3a**−**y**[a]

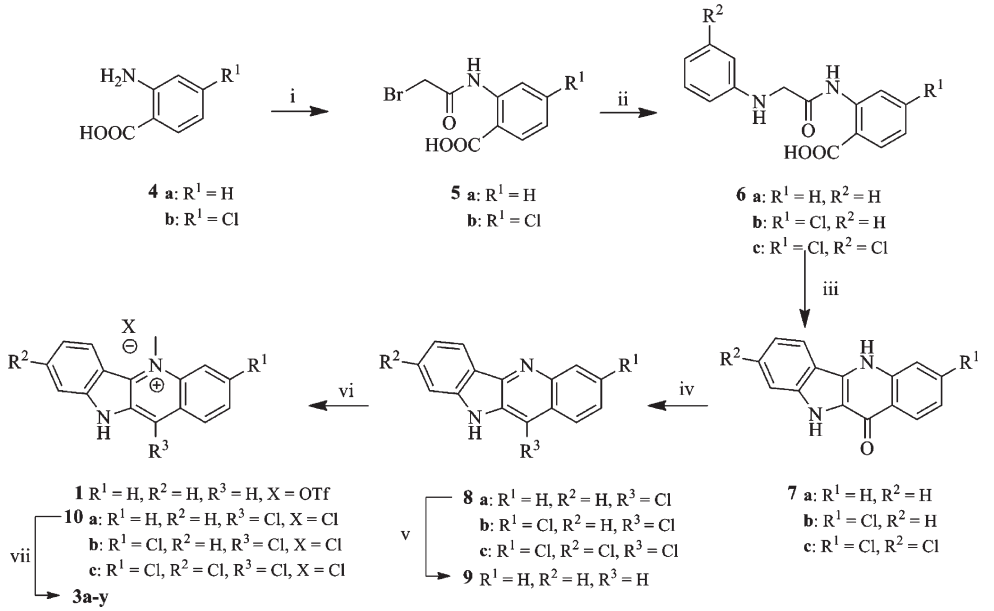

[a] Reagents and conditions: (i) bromoacetyl bromide, DMF/1,4-dioxane (1:1), rt; (ii) aniline, DMF, 100 °C; (iii) PPA, 130 °C; (iv) $POCl_3$, 130 °C; (v) H_2 Pd−C 10% NaOAc, AcOH, 60 psi; (vi) (a) **8** or **9**, methyl triflate, toluene, rt, (b) HCl in ether for **8**; (vii) NH_2-linker-NR^4R^5, AcOEt, reflux.

and subsequent reduction with $NaBH_3CN$ in 59, 66, and 30% yields, respectively (Scheme 2).

For derivatives **3d**, **3j**, **3l**, and **3t**, it was necessary to synthesize the corresponding diamines required for the substitution reaction with **10**. Thus, N^1,N^1-dimethylpropane-1,2-diamine, **12**, used for the synthesis of **3d**, was prepared by reductive amination of *N*,*N*-dimethylaminopropanone, **11**, with ammonium acetate and $NaBH_3CN$ (Scheme 3). 3-(Piperidin-1-yl)propan-1-amine, **15**, required for the synthesis of **3j**, was prepared via Gabriel synthesis, using phthalimide **13** as starting material (Scheme 3). N^1,N^1-Diethylbutane-1,4-diamine, **18**, required for the synthesis of **3l**, was prepared by reductive alkylation of **16** with acetaldehyde and $NaBH_3CN$, followed by removal of the Boc group with triflouroacetic acid (Scheme 3). Compound **3t** was synthesized by reaction of **10a** with acetamide, **20**, which was obtained by Mannich reaction of phenol **19** with formaldehyde and diethylamine (Scheme 3).

Structures of all compounds **3a**−**y** were established on the basis of two-dimensional ^1H and ^{13}C heterocorrelation NMR experiments (HMQC and HMBC) and the position of the side chain at C11 was confirmed by NOE difference experiments. Figure 2 provides an example of such NOE connectivities detected for **3h** in the NMR experiments, which shows a $^1H-^1H$ connectivity between the side chain methylene group adjacent to *NH*-C11 (δ_H 4.21 ppm) with the proton of the indole nitrogen (δ_H 10.75 ppm), as well as the protons at δ_H 4.56 ppm from the *N5*-CH_3 group with doublets at δ_H 8.33 and 8.51 ppm, assigned to aromatic protons at C4 and C6, respectively. Cryptolepine analogues **3** showed also a shielding effect on ^1H chemical shifts of *N5*-CH_3 of 0.1−0.45 ppm when compared with **10**. Additionally, the ^{13}C chemical shifts of C10a and C11a showed an upfield shift of the order of 10 ppm and of 3 ppm for *N5*-CH_3, when compared with **1** and **10**, whereas the chemical shift of C11 showed a deshielding effect of 10−15 ppm when compared with the parent compounds **1** and **10**.

Scheme 2. Synthesis of Cryptolepine Analogues **3o**−**q**[a]

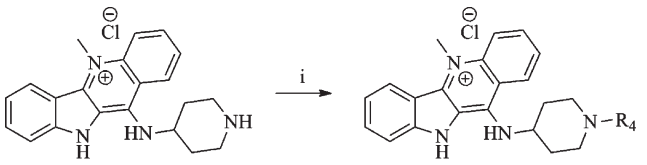

3n

3o: R^4 = isobutyl
p: R^4 = benzyl
q: R^4 = 2-hydroxybenzyl

[a] Reagents and conditions: (i) Bu^iCHO, $PhCH_2CHO$ or 2-OH-C_6H_4CHO, anhydrous Na_2SO_4, $NaBH_3CN$, dry MeOH, rt, 24 h.

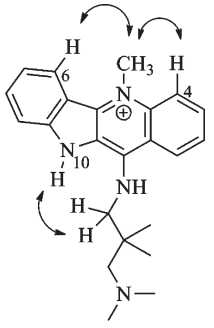

Figure 2. NOE correlations observed for cryptolepine derivative **3h** in the NMR experiments.

Scheme 3. Synthesis of Amines **12**, **15**, **18**, and **20**[a]

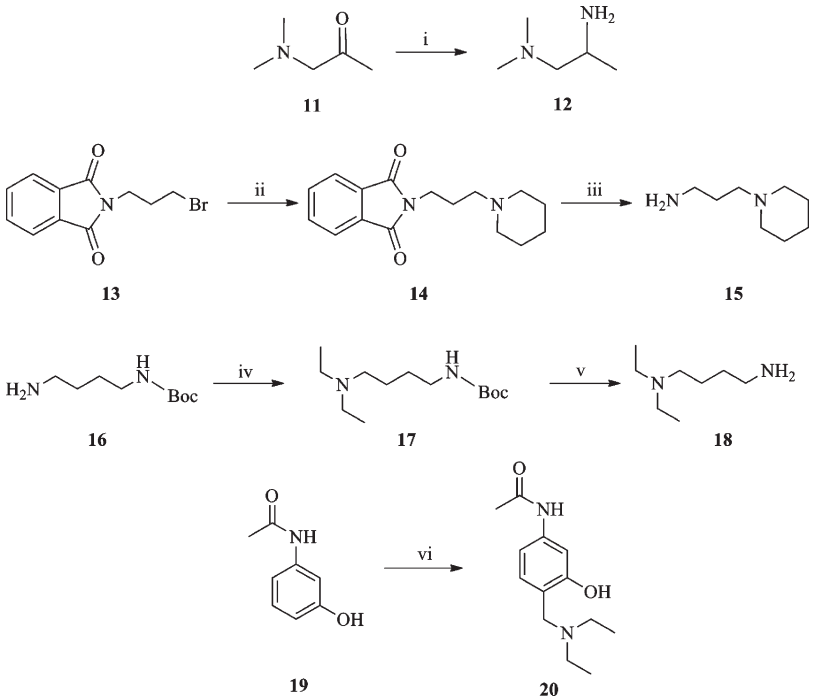

11 **12** **13** **14** **15** **16** **17** **18** **19** **20**

[a] Reagents and conditions: (i) NH_4OAc, $NaBH_3CN$, anhydrous $MgSO_4$, dry MeOH, reflux; (ii) piperidine, triethylamine, CH_2Cl_2, reflux; (iii) hydrazine; (iv) MeCHO, anhydrous $MgSO_4$, $NaBH_3CN$, dry MeOH, 0 °C, 2h; (v) CH_2Cl_2:TFA (1:1), rt, 1 h; (vi) aq HCHO, diethylamine, EtOH, reflux, 96 h.

Table 1. In Vitro Antiplasmodial Activity (IC_{50}) against *P. falciparum* W2, V1/S, 3D7, and D6 Strains, Cytotoxicity (IC_{50}) against Vero Cells, Selectivity Index (SI), and Resistance Index (RI) of Chloroquine (**2**), Cryptolepine (**1**) and Derivatives (**3a**−**y**)

Comp	R^1	R^2	R^3	*In vitro* antiplasmodial activity IC_{50} (nM)				IC_{50} *Vero* cells (μM)	SI[a]	RI[b]
				W2	V1/S	3D7	D6			
CQ (2)	--	--	--	138±16	89±31	5.5±0.3	14.2±0.3	--	--	25
1	H	H	H	755±1	424±78	259±29	222±5	1.05±0.03	1.4	2.9
3a	H	H		89±8	115±68	156±40	107±10	60±20	678	0.6
3b	H	H		50±8	62±3	85±26	66±8	5.5±0.5	111	0.8
3c	H	H		82±23	130±18	72±1	70±5	2.8±0.5	34	1.2
3d	H	H		142±2	202±47	165±25	78±5	3±1	23	0.9
3e	H	H		26±5	54±16	133±3	71±10	10±4	371	0.2
3f	H	H		20±1	24±2	51±1	46±5	2.2±0.04	109	0.4
3g	H	H		32±5	20±8	29±3	32±2	2.5±0.3	78	1.1
3h	H	H		184±21	146±22	144±6	250±25	3±1	18	1.3
3i	H	H	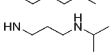	22±2	26.1±0.6	28±1	34±1	3±1	125	0.8
3j	H	H	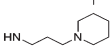	36±2	23±9	28±7	34±5	2.0±0.3	56	1.3
3k	H	H	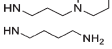	65±1	190±59	422±15	245±71	>85	1307	0.2
3l	H	H	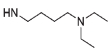	29±2	22.3±0.4	66±7	71±2	10±3	358	0.4
3m	H	H	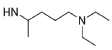	122±3	145±5	274±25	161±9	13±5	103	0.4
3n	H	H		44±1	23±5	60±12	59±1	62±9	1408	0.7
3o	H	H	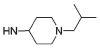	70±1	70±34	76±1	86±25	5±1	70	0.9
3p	H	H	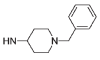	108±19	56±16	59±2	86±15	2.2±0.1	21	1.8
3q	H	H	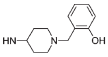	276±31	536±7	418±76	185±29	2.6±0.7	10	0.7
3r	H	H		265±70	291±241	128±2	154±29	0.6±0.2	2	0.2
3s	H	H	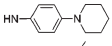	455±18	375±56	176±17	287±67	4.83±0.07	11	2.6
3t	H	H	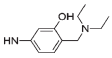	52±1	56±22	15±2	24±1	0.8±0.3	17	3.5
3u	H	H		180±14	247±34	279±71	166±2	2.6±0.6	14	0.6
3v	Cl	H	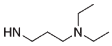	21±1	34±15	40±12	70±9	1.3±0.4	60	0.5
3w	Cl	H		45±1	65±4	52±4	70±16	4.4±0.2	98	0.9
3x	Cl	Cl		48±6	31±12	35±4	30±2	0.8±0.3	16	1.4
3y	H	H		1252±98	2205±689	1773±70	1289±69	3±2	2	0.7

[a] Selectivity index toward W2 strain, which is expressed by the ratio $IC_{50}^{Vero}/IC_{50}^{W2}$. [b] Resistance index, which is expressed by the ratio $IC_{50}^{W2}/IC_{50}^{3D7}$.

Results and Discussion

Antiplasmodial Activity. Cryptolepine, **1**, and derivatives **3a**−**y** were evaluated for their antiplasmodial activity against a panel of *P. falciparum* strains with different drug resistance phenotypes: W2 (chloroquine-resistant), 3D7 (chloroquine-sensitive), V1/S (chloroquine- and pyrimethamine-resistant), and D6 (chloroquine-sensitive, mefloquine-resistant) (Table 1). Cryptolepine was 2- to 3.5-fold more active against the CQ-sensitive than the CQ-resistant strains, with resistance index (RI), as expressed by the ratio $IC_{50}^{W2}/IC_{50}^{3D7}$, of about 3. More importantly, cryptolepine derivatives containing a secondary or tertiary terminal basic amine (e.g. **3b**, **3f**, **3g**, **3i**, **3j**, and **3n**) were shown to be potent antiplasmodials, with IC_{50} values generally of 20−90 nM (Table 1). These results indicate that the diaminoalkane side chain, when attached to C-11 of the indolo[3,2-*b*]quinoline, leads to potent compounds against both CQ-sensitive and CQ-resistant strains. The exception seems to be derivatives **3** containing a terminal primary amine, as these compounds displayed reduced activity, particularly against 3D7 and D6 strains, when compared with compounds with secondary (**3e** vs **3i**) or tertiary terminal amines (e.g., **3a** vs **3c**, **3e** vs **3g** and **3k** vs **3l**). The reason for these differences in activity is not obvious, and an extended evaluation of terminal amines will be necessary to further understand the loss of potency in compounds **3** with a terminal primary amine. Additional evidence for the importance of a basic distal amine for antiplasmodial activity comes from the observation that compound **3y** which lacks a distal basic amine group is weakly active, with IC_{50} values of 1299−2200 nM against CQ-sensitive and CQ- resistant strains.

A comparison of the different linkers between the distal basic center and the indolo[3,2-*b*]quinoline moiety reveals

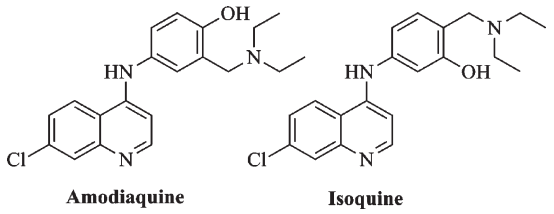

Figure 3. Structures of amodiaquine and its isomer isoquine.

that compounds **3** containing a propyl or butyl linear side chain are slightly more potent than their ethyl counterparts. For example, the *N*,*N*-diethylaminopropyl and *N*,*N*-diethylaminobutyl derivatives, **3g** and **3l**, are approximately 2.5 times more potent than their ethyl counterpart, **3c**, against the CQ-resistant W2 strain. These results are consistent with reports that 4-aminoquinoline analogues with shortened side-chains retain activity against CQ-resistant strains, although no major difference in activity has been observed between the ethyl and propyl linkers.[29,30]

Branched linkers lead to a significant reduction in antiplasmodial activity when compared with their linear counterparts (e.g., **3d** vs **3b** and **3h** vs **3f**−**g**,**i**−**j**). Furthermore, compound **3m**, containing a side chain identical to that of chloroquine, displayed reduced activity against both CQ-resistant and CQ-sensitive *P. falciparum* strains (IC_{50} ranging from 120 to 275 nM), being 2- to 6-fold less potent than its linear butyl counterpart **3l**. These results are in line with the observation that 4-aminoquinolines containing the chloroquine side chain give consistently lower potency than those with a propyl side chain against both 3D7 and W2 strains.[31] Compound **3n**, with a piperidine side-chain, was highly active against both CQ-resistant and CQ-sensitive strains, suggesting that a conformational constraint between the distal basic center and the indolo[3,2-*b*]quinoline scaffold may improve potency. Appending a sterically demanding *iso*-butyl or benzyl group to the nitrogen atom of the piperidine moiety (**3o** and **3p**, respectively) did not significantly alter antiplasmodial activity. To our surprise, the derivative containing a 2-hydroxybenzyl group, **3q**, was 2- to 10-fold less active than its benzyl counterpart, **3p**. In contrast, compound **3t**, which contains a 2-diethylaminomethylphenol moiety, exhibited IC_{50} values of ca. 20 and 54 nM against the CQ-sensitive and CQ-resistant strains, respectively. The 2-diethylaminomethylphenol and related α-aminocresol motifs are commonly found in potent antimalarials such as amodiaquine and its isomer isoquine (Figure 3),[32−34] and it has been postulated that intramolecular hydrogen bonding between the protonated amine (H-bond donor) and the hydroxyl (H-bond acceptor) may be an important feature for activity against CQ-resistant *P. falciparum* strains.[35]

The 3-chloro and 3,8-dichloro derivatives, **3w** and **3x**, respectively, were equipotent ($IC_{50} \approx 45$ nM) with their unsubstituted counterpart, **3n**, against the panel of CQ-sensitive and CQ-resistant strains, suggesting that introduction of electron-withdrawing substituents in the indolo[3,2-*b*]-quinoline moiety does not significantly affect antiplasmodial activity when a diaminoalkane side-chain is present at C11. Interestingly, it has been reported that 3-chlorocryptolepine is equipotent with cryptolepine against the *P. falciparum* K1 strain, while its 8-chloro counterpart is inactive.[36] In contrast, 2,8-dichlorocryptolepine was found to be 10-fold more potent than cryptolepine in the same screen.[11,36]

Anti-*Plasmodium* Liver Stage Activity. Cryptolepine and derivative **3n** were also assessed against liver stages of the rodent malaria parasite *Plasmodium berghei* at a concentration of 5 μM, using a recently described fluorescence activated cell sorting (FACS)-based method.[37] This method is based on the measurement of the fluorescence of Huh-7 cells, a human hepatoma cell line, following infection with GFP-expressing *P. berghei* sporozoites. Both compounds were inactive in this assay, a result that points toward the selectivity of **1** and derivatives **3** for erythrocytic stages of malaria parasites.

Cytotoxicity. The in vitro cytotoxicity of compounds **3a**−**y** and cryptolepine was evaluated using mammalian *Vero* cells. Remarkably, most of the derivatives **3a**−**y** were less cytotoxic than the parent compound, with **3a**, **3k**, and **3n** being 60- to 85-fold less cytotoxic than cryptolepine (Table 1). Moreover, a comparison of selectivity index (SI) results, as expressed by the ratio $IC_{50}{}^{Vero}/IC_{50}{}^{W2}$, reveals that compounds **3** with a terminal primary amine (i.e., **3a**, **3e**, and **3k**, and with the butyl and piperidine side-chains (**3l** and **3n**, respectively) were significantly more selective than the parent compound. The presence of chlorine atoms in the indolo-[3,2-*b*]quinoline led to an increase in cytotoxicity when compared to the unsubstituted counterpart, **3n**. Incorporation of isoquine's α-aminocresol motif at C-11 (i.e., **3t**), resulted in a cytotoxicity level comparable to that of cryptolepine, despite the improvement in SI.

Distribution into *P. falciparum*-Infected Erythrocytes. Cryptolepine, **1**, was previously reported to accumulate in the nucleus of schizont-infected erythrocytes, which led to the conclusion that cryptolepine interferes with the parasite's replication at schizont stage due to its DNA intercalating ability.[23] To investigate the possible sites of action of newly synthesized cryptolepine analogues **3**, the intracellular distribution of **3n** in blood stages of *P. falciparum* was studied by fluorescence microscopy and compared with that of **1**. Figure 4 shows the contrast phase and fluorescence images of *P. falciparum*-infected erythrocytes after incubation of *P. falciparum* cultures with the compounds. Our data shows that **1** and its derivative **3n** accumulate inside erythrocytic ring-stage parasites and the observed intensity of fluorescence indicates that nucleus and food vacuole are parasite organelles targeted by both compounds. It should be noted that hematin very efficiently quenches the fluorescence of cryptolepine derivative **3n**, which results in around 60% quenching of fluorescence intensity for a 1:1 ligand:hematin ratio, while DNA only quenches 20% the fluorescence of **3n** (Figures S3 and S4, Supporting Information). Quenching by hematin has also been reported for the fluorescence of acridine conjugates.[38] These results suggest that quenching of **3n** in the food vacuole may occur as a result of the presence of hematin, thus underestimating the vacuolar signal when compared with the nonvacuolar signal arising from accumulation in the nucleus. Overall, this data indicates that incorporation of basic side chains into the cryptolepine structure does not notably promote selective accumulation of cryptolepine analogues toward acidic digestive vacuole of the parasite.

Binding to a Double-Stranded Oligonucletide. The observation that compounds **3** can accumulate in the nucleus prompted us to explore alternative targets for their antiplasmodial activity and study their binding properties toward DNA using a 12-mer double-stranded $d(GATCCTAGGATC)_2$ oligonucleotide as a model system. This self-complementary oligonucleotide was preferred over larger double-stranded structures in order to avoid multiple binding modes that

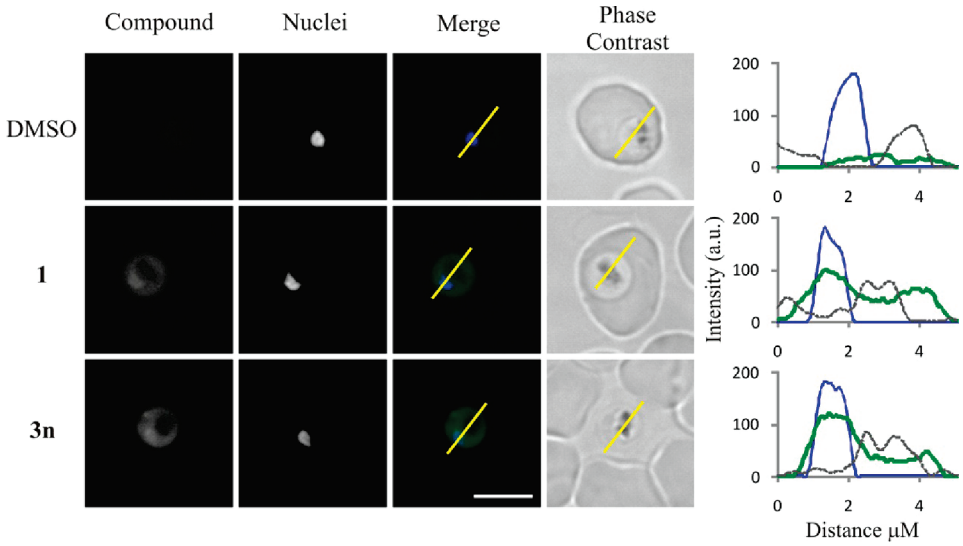

Figure 4. Intracellular localization of **1** and **3n** in *P. falciparum*-infected erythrocytes. Cells were incubated for 3 h at room temperature, in the dark, with 5 μM of cryptolepine and its analogue **3n** and immediately observed using a Zeiss Axiovert 200 M fluorescence microscope after being washed with PBS. The yellow lines indicate the regions corresponding to the plot profiles on the right. Green, compounds **1** or **3n**; blue, nuclei; gray line, digestive vacuole (phase contrast image).

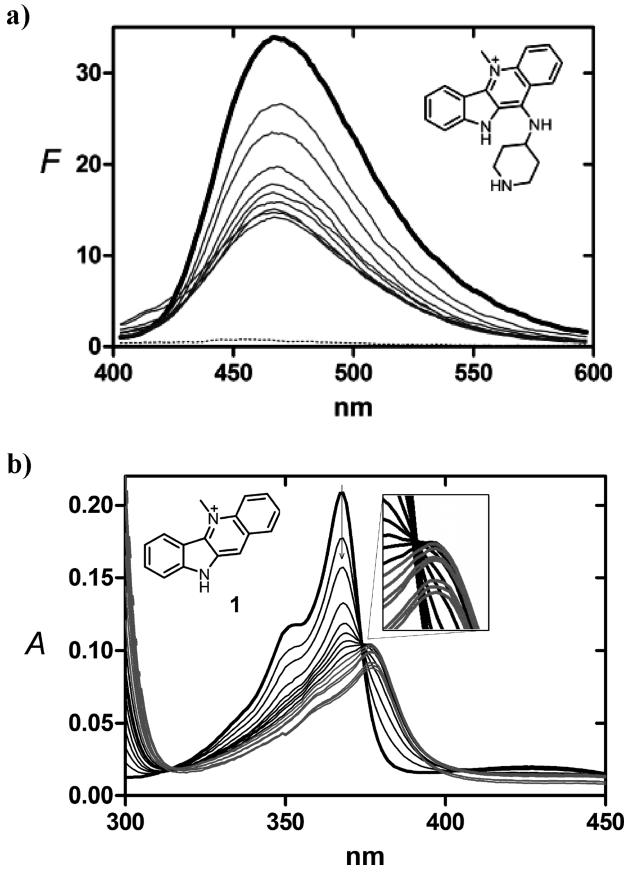

Figure 5. Fluorescence and UV−visible spectral changes at 25.0 °C upon titration of **3n** and cryptolepine with the 12-mer DNA duplex d(GATCCTAGGATC)$_2$ in 0.01 M phosphate buffer at pH 7.40 containing 0.1 M NaCl. (a) Fluorescence emission spectra of **3n** (5 μM). The DNA:ligand ratio increased as follows: 0, 0.3, 0.5, 0.8, 1.1, 1.6, 2.1, 2.6, and 3.1 sequentially from the top spectrum. (b) UV−visible spectra of **1** (5 μM). The DNA:ligand ratio increased as follows: 0, 0.2, 0.5, 1.0, 1.6, 2.1, 2.6, 3.1, 4.0, 5.0, 6.4, 7.6, 8.8, 10.2, 11.3 and 12.3, sequentially from the top spectrum. The expanded box shows details in the region of the 374 nm isosbestic point.

could preclude the determination of binding constants accurately.

The equilibrium association constants of cryptolepine derivatives **3a**−**y** binding to d(GATCCTAGGATC)$_2$ in phosphate buffer containing 0.1 M NaCl and at 25 °C were determined by spectrofluorometry. All emission spectra were recorded at an excitation wavelength of 339 nm. Emission of compounds **3** in aqueous solutions was characterized by broad band at ca. 460 nm, and its fluorescence intensity was proportional to their concentrations up to 20 μM, indicating that there was no significant intermolecular stacking which would give rise to a quenching effect. The fluorescence titration spectra of compounds **3a**−**y** (see Figure 5a for **3n** as an example) showed shifts of 5−10 nm and up to 60% quenching of fluorescence intensity on addition of the oligonucleotide, thus indicating the formation of a complex. The plots of the change in the fluorescence intensity (see Supporting Information), corrected for dilution, vs the concentration of the oligonucleotide added were fitted by the equation for a single-site binding (eq 1),

$$F = F_{max}[\mathrm{DNA}]/(K_d + [\mathrm{DNA}]) \quad (1)$$

where F is the observed value of emission intensity, F_{max} its limiting value at high values of [DNA], and K_d the dissociation constant. The equilibrium association constants, K_{ass}, were determined as the inverse of K_d (eq 2),

$$K_{ass} = 1/K_d \quad (2)$$

For compounds **3e**, **3j**, **3m**−**n**, **3q**−**t**, and **3x**−**y**, there was also evidence of an additional, much weaker binding site, as revealed by a continuous, but very small, increase in the fluorescence intensity at high concentration of oligonucleotide (see Supporting Information). In these cases, the plots of fluorescence intensity vs [DNA] were fitted by the simplified equation for two independently acting binding sites (eq 3),

$$F = (\{F_{max}[\mathrm{DNA}]/(K_d + [\mathrm{DNA}])\} + C[\mathrm{DNA}]) \quad (3)$$

where $C = F'_{max}/K'_d$, and K'_d is the dissociation constant for the weaker process (see Experimental Section). The equilibrium

Table 2. Association Constants, K_{ass}, for Binding of Cryptolepine Derivatives **3** to d(GATCCTAGGATC)$_2$ (ds-DNA) and Heme, along with IC_{50} Values for the Inhibition of Falcipain-2 (FP-2) and -3 (FP-3)

compd	ds-DNA K_{ass}($\times 10^6$ M^{-1})	heme binding K_{ass}($\times 10^6$ M^{-1})	FP-2 IC_{50} (μM)	FP-3 IC_{50} (μM)	compd	ds-DNA K_{ass} ($\times 10^6$ M^{-1})	heme binding K_{ass}($\times 10^6$ M^{-1})	FP-2 IC_{50} (μM)	FP-3 IC_{50} (μM)
1	0.25 ± 0.01[a]	0.045 ± 0.003	38 ± 9	> 50	**3m**	4.3 ± 0.2[b]	0.062 ± 0.07	11.6 ± 0.2	7 ± 2
3a	0.85 ± 0.01[b]	0.127 ± 0.007	6.3 ± 0.2	> 25	**3n**	0.74 ± 0.03[b]	0.154 ± 0.006	6.39 ± 0.04	7.9 ± 0.5
3b	3.1 ± 0.7[b]	0.120 ± 0.005	> 50	ND[c]	**3o**	0.74 ± 0.07[b]	0.227 ± 0.008	10.5 ± 0.6	16 ± 2
3c	1.14 ± 0.05[b]	0.41 ± 0.03	> 50	ND	**3p**	0.68 ± 0.09[b]	0.125 ± 0.007	12.8 ± 0.9	ND
3d	1.9 ± 0.1[b]	0.148 ± 0.008	8.3 ± 0.5	14 ± 1	**3q**	0.6 ± 0.3[b]	0.108 ± 0.005	14.8 ± 0.2	43 ± 6
3e	0.25 ± 0.01[b]	0.18 ± 0.02	11 ± 1	14 ± 1	**3r**	0.51 ± 0.06[b]	0.155 ± 0.008	14 ± 2	ND
3f	3.0 ± 0.2[b]	0.066 ± 0.005	34 ± 5	> 50	**3s**	3.4 ± 0.6[b]	0.21 ± 0.02	8.2 ± 0.2	ND
3g	9.1 ± 0.6[b]	0.127 ± 0.007	ND	ND	**3t**	0.8 ± 0.3[b]	0.075 ± 0.009	15.2 ± 0.9	ND
3h	2.6 ± 0.4[b]	0.069 ± 0.007	33.5 ± 0.8	26 ± 7	**3u**	1.0 ± 0.1[b]	0.17 ± 0.01	9.32 ± 0.09	ND
3i	5.0 ± 0.8[b]	0.20 ± 0.01	> 25	ND	**3v**	17 ± 1[b]	0.11 ± 0.01	11 ± 1	ND
3j	5.3 ± 0.3[b]	0.161 ± 0.008	ND	ND	**3w**	4.5 ± 0.4[b]	0.18 ± 0.01	5.6 ± 0.1	ND
3k	1.4 ± 0.1[b]	0.147 ± 0.006	ND	ND	**3x**	1.6 ± 0.4[b]	0.12 ± 0.01	4.8 ± 0.3	ND
3l	9 ± 1[b]	0.15 ± 0.01	ND	ND	**3y**	0.47 ± 0.06[b]	0.19 ± 0.01	18 ± 2	46.3 ± 0.8

[a] UV−visble spectroscopy determination. [b] Fluorescence spectroscopy determination. [c] ND: not determined.

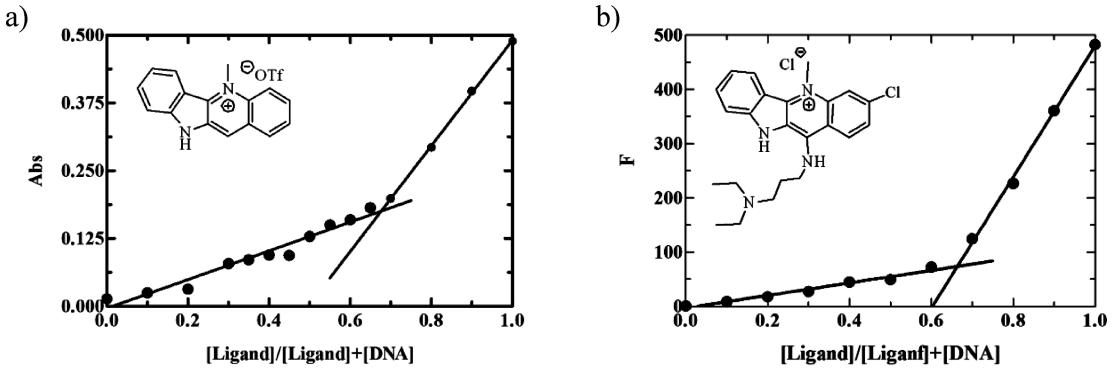

Figure 6. Job plots for (a) **1** and (b) **3v** complexed with 12-mer d(GATCCTAGGATC)$_2$ oligonucleotide at 0.01 M phosphate buffer (pH 7.4), containing 0.1 M NaCl, at 25 °C. The sum of the concentrations of ligand and oligonucleotide was kept constant at 12.5 μM for **1** and 2.5 μM for **3v**. For **1**, absorbance was measured at 368 nm, and for **3v**, fluorescence was measured at 483 nm with excitation at 339 nm.

association constants, K_{ass}, for compounds **3a**−**y** are presented in Table 2.

The spectrofluorometric assay failed with cryptolepine triflate salt, **1**, because no quenching was observed with increasing concentrations of oligonucleotide, and thus binding of cryptolepine to the DNA duplex d(GATCCTAGGATC)$_2$ was assessed by UV−visible spectroscopy. The spectral changes of triflate salt of **1** showed bathochromic and hypochromic shifts upon addition of oligonucleotide duplex (Figure 5b). Sharp isosbestic points were present at 374 and 405 nm for oligonucleotide/ligand ratios from 0 to 2.6, indicating a relatively strong binding of the triflate salt **1** to d(GATCCTAGGATC)$_2$. Further increases in oligonucleotide concentration caused a shift in the isosbestic point, suggesting a second, weaker binding process at higher oligonucleotide concentrations. This result is consistent with two independent and noncooperative types of binding as previously reported for cryptolepine.[40]

Job plot analysis[41,42] was performed to measure the stoichiometry of association of cryptolepine and its derivative showing the highest K_{ass}, **3v**, with d(GATCCTAGGATC)$_2$ in 0.01 M phosphate buffer at pH 7.40 containing 0.1 M NaCl. The maximum absorbance for **1** and **3v** as a function of the mole fraction of ligand was plotted to give linear dependences at high and low molar fractions (Figure 6). The stoichiometry of the formed complex was determined by the intersections of these lines. These intersections at ligand mole fractions of 0.67 (for **1**) and 0.66 (for **3v**) suggests a ligand:oligonucleotide ratio of 2:1 for both complexes. The 2:1 stoichiometry for the cryptolepine:oligonucleotide complex detemined in this research is consistent with the previously reported crystal structure of cryptolepine:d(CCATGG)$_2$, in which cryptolepine molecules were stacked between the duplexes as well as at each extremity of the double-hexamer duplex and intercalated in two CC sites.[12]

To obtain a better insight into the nature of the interaction with the double-stranded oligunucleotide, titrations were also performed at a higher ionic strength. Titration of **1** with d(GATCCTAGGATC)$_2$ was performed in 0.01 M phosphate buffer (pH 7.4) containing 1 M NaCl. The increased concentration of Na^+ counter cations resulted in a K_{ass} value of 1.0 ($\pm$0.1) $\times$ 10^5 M^{-1}, which is of the same order of magnitude as that determined in phosphate buffer containing 0.1 M NaCl (Table 2). As expected, **1** maintains its binding capabilities to the double-stranded oligonucleotide at high ionic strength solutions, consistent with intercalation.[43,44] In contrast, no interaction was observed between **3n** and **3t** with the DNA duplex d(GATCCTAGGATC)$_2$ in phosphate buffer containing 1 M NaCl. This remarkable loss of binding in the presence of high concentration of Na^+ counter cations strongly suggests that binding properties of derivatives **3** to the oligonucleotide duplex are largely dependent on electrostatic interactions between the two species, which can be attributed to the interactions between the protonated primary, secondary, or tertiary amine groups **3a**−**y** and negatively charged sugar−phosphate backbones of the DNA

duplex. This data provides an evidence that incorporation of a basic side chain into cryptolepine structure alters to a certain extent the mode of interaction of the ligand with the DNA duplex by adding electrostatic component to that, which seem to become highly essential, and might be linked to the enhanced antiplasmodial activity seen for the cryptolepine analogues.

From the data in Table 2, K_{ass} values for cryptolepine derivatives **3a**−**y** span almost 2 orders of magnitude, ranging from 0.25 to 17 × 10^6 M^{-1}. Overall, these derivatives interact more strongly with the oligonucleotide than cryptolepine. Interestingly, the K_{ass} values also compare favorably with that of chloroquine, which has been recently reported to bind to DNA with a K_{ass} value of ca. 10^5 M^{-1}.[39] Inspection of Table 2 shows that compounds **3** containing linear side chains with a distal tertiary or secondary amine generally display higher binding affinities toward the oligonucleotide than those with a terminal primary amine (e.g., **3g** vs **3e** and **3l** vs **3k**), a trend similar to that observed with antiplasmodial activity (Table 1). There appears to be no clear correlation between the in vitro cytotoxicity and the binding of compounds **3** to the oligonucleotide based on measured the corresponding K_{ass} values. In an attempt to understand the observed structure-binding relationships, molecular properties of selected cryptolepine derivatives **3** were studied by density functional theory (DFT; see Supporting Information). However, no clear-cut correlations emerged between molecular parameters such as the atomic charges at *N*-10 and *N*-5 of **3** and the corresponding K_{ass} values and thus this matter requires further detailed investigations in a separate study.

Hematin Binding Studies. Taking in account that (i) the antiplasmodial mechanism of cryptolepine is likely to be due, at least in part, to inhibition of hemozoin formation[19] and (ii) the fluorescence microscopy study could not rule out distribution of compounds **3** into the digestive vacuole of the parasite, we decided to evaluate the binding of compounds **3** to hematin.

The equilibrium binding constants (K_{ass}) with hematin monomer (FPIX-OH) were determined by UV−visible titration carried out in pH 5.5 buffer containing 40% DMSO v/v to minimize porphyrin aggregation and μ-oxo dimer formation.[34,45−48] Spectral changes at the FPIX-OH Soret band (λ = 402 nm)[49,50] were recorded, and the resulting absorbance data were first corrected for dilution and then analyzed using GraphPad nonlinear curve fitting software. Several binding processes have been considered for fitting the data from quinoline and acridine antimalarials, the most successful corresponding to (i) 1:1 association between drug and FPIX-OH (model 1), (ii) 2:1 association of drug to FPIX-OH in a stepwise fashion (model 2), and (iii) 1:2 stepwise association of drug to FPIX-OH (model 3).[49,51,52] The best fit of absorbance data from compounds **3a**−**y** and cryptolepine was obtained with model 1 (Supporting Information), and the resulting log K_{ass} values are presented in Table 2. The 1:1 binding stoichiometry as determined by titration was confirmed using the continuous variation technique (Job's plot)[41,42] for cryptolepine, chloroquine and **3c**, changing the FPIX-OH molar ratio and maintaining the sum of the concentrations of the ligand and FPIX-OH constant at 10 μM. The Job's plots in Figure 7a−c show 1:1 complex formation for cryptolepine, chloroquine, and **3c**, respectively. Titration with chloroquine was also performed for comparison purposes, but in this case, both binding models 1 and 3 gave excellent fits to the absorbance data (r^2 of 0.997 and 0.999, respectively). The Job's plot for chloroquine shows that

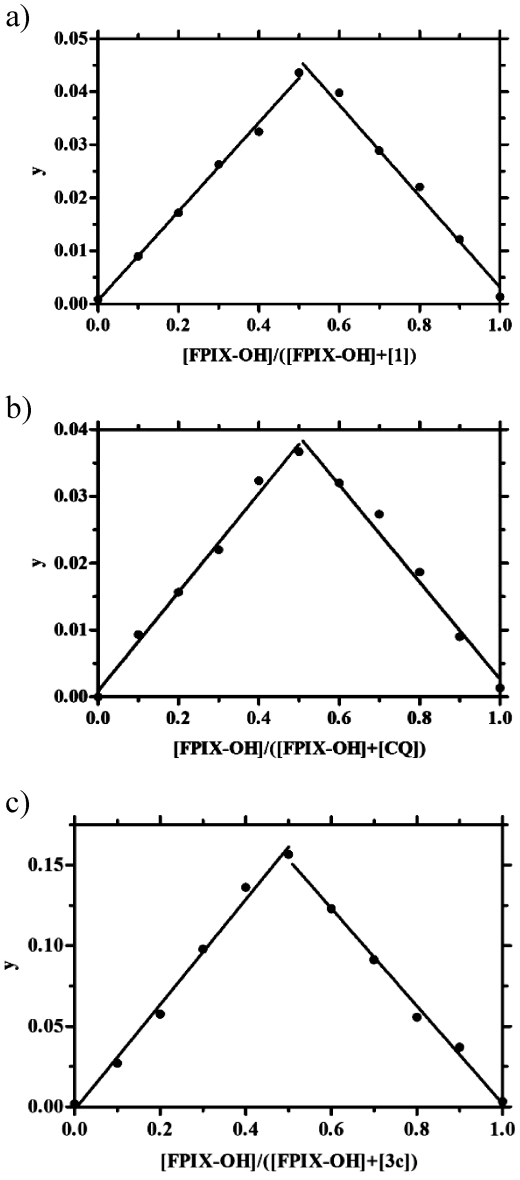

Figure 7. Job plots for (a) cryptolepine (**1**), (b) chloroquine (**2**), and (c) derivative **3c** with FPIX-OH in buffered 40% DMSO v/v, pH 5.5 at 25 °C.

the intercept occurs at a molar ratio of 0.51, i.e. consistent with 1:1 binding stoichiometry (Figure 7b). This result is in line with the observation of Egan and co-workers that the 1:1 complex is the predominant species in pH 7.5 buffer containing 40% DMSO, while the 1:2 complex is likely to occur only at lower ratios of chloroquine to FPIX-OH.[49]

Inspection of Table 2 shows that K_{ass} values for **3a**−**y** range from 0.062 to 0.227 × 10^6 M^{-1}, while the K_{ass} value for cryptolepine is 0.045 × 10^6 M^{-1}, indicating that introduction of a side-chain at C-11 of the cryptolepine aromatic nucleus increases the interaction with FPIX-OH when compared with the parent compound. Importantly, the K_{ass} values for **3a**−**y** compare favorably to that of chloroquine (0.085 × 10^6 M^{-1} in our assay), indicating that cryptolepine analogues **3** share with chloroquine the ability to interact with hematin monomer. Interestingly, the phenyl derivative **3r** binds as efficiently as most of the derivatives containing a terminal basic group to hematin monomer, which suggests that a distal basic amine is not an absolute requirement for binding.

It should be noted that chloroquine can also inhibit hemozoin crystal growth by binding to its crystal faces.[22] According to this hemozoin crystal growth model, the flat and well exposed face of the crystal shows repeats of propionic carboxylate groups separated by 8.0 Å, which may be the target of positively charged groups.[21] Remarkably, we found that the distances between the positively charged *N*-5 nitrogen atom and the distal amine groups of piperidine (**3n**), propyl (**3f**), and butyl (**3l**) derivatives are ≈8 Å (Supporting Information), a value consistent with binding to the hemozoin crystal flat face.

Inhibition of Cysteine Proteases Falcipain-2 and -3. Cryptolepine derivatives **3** were also screened for inhibition of cysteine proteases from *P. falciparum*, falcipain-2 (FP-2) and -3 (FP-3) (Table 2), which are of particular interest as therapeutic targets due to their role in parasite development.[53] Both FP-2 and FP-3 are involved in the hydrolysis of host hemoglobin in the parasite's digestive vacuole, and falcipain inhibitors have been reported to block the development of cultured erythrocytic parasites[54] and to cure mice infected with lethal malaria infections.[55] Inspection of the data in Table 2 shows that compounds **3** are poor to moderate inhibitors of FP-2 and FP-3. The IC_{50} values against FP-2 ranged from 4.8 μM for the dichloro derivative **3x** to 34−50 μM for derivatives incorporating linear or branched alkylamine side chains. Furthermore, compounds **3** generally display only moderate selectivity toward FP-2 when compared to FP-3. The observation that falcipains are inhibited only in the μM range, suggests that the indolo[3,2-*b*]quinoline is not suitable for enzyme binding and that falcipains cannot be considered as the main targets for cryptolepine derivatives **3**.

Conclusion

On the basis of previous reports indicating that a basic amino side-chain is a major requirement for chloroquine accumulation in the acid digestive vacuole of the parasite, we synthesized a series of cryptolepine analogues containing diaminoalkane side chains (−NH-linker-NR^1R^2) at C-11 with the initial aim to facilitate localization of these ligands within the plasmodial vacuole. These novel cryptolepine derivatives were obtained by reaction of the key intermediate, 11-chlorocryptolepine, with the appropriate amine, to give moderate to good yield.

A major outcome of this work is that several cryptolepine analogues with a diaminoalkane side hain at C-11 position showed significant increase of the antiplasmodial activity against both CQ-resistant and CQ-sensitive *P. falciparum* strains when compared with the parent compound and with the currently used antimalarial drug chloroquine. Maximum potency was achieved with propyl and butyl side chains, while branched linkers seemed to be poorly tolerated. More importantly, some of these identified agents (e.g., **3e**, **3f**, **3i**, **3k**, **3l**, and especially **3n**) combine significant antiplasmodial activity with a very low cytotoxicity. The cytotoxicity profile was particularly improved for the derivative containing a conformationally restricted piperidine side-chain, **3n**, displaying a selectivity index value of ca. 1400, i.e. a 1000-fold increase compared with the parent compound.

The research was also focused on identification of possible biological targets for this new class of antimalarial agents in order to understand an origin of this substantial improvement in potency and selectivity against *P. falciparum* strains. Fluorescence microscopy revealed that these cryptolepine derivatives accumulate inside the nucleus and, to some extent, in the digestive vacuole of blood stages of parasite. These data clearly indicated that incorporation of a diaminoalkane side chain, as a strategy that has been extensively used as a pH-trapping device in antimalarial drug design, was not sufficient enough to provide cryptolepine derivatives with the ability to accumulate selectively in the digestive vacuole. Instead, there seem to be some other mechanisms which effectively promote antimalarial activity of the studied analogues. Indeed, it was demonstrated that compounds **3a**−**y** generally displayed enhanced association constants toward the double-stranded oligonucleotide duplex, presumably due to additional electrostatic interactions with the negatively charged sugar−phosphate backbones, which might be linked to the improved antiplasmodial activity via inhibition of parasite DNA replication.[22] The interactions between the cryptolepine analogues and hematin could be an additional mechanism of antiplasmodial activity seen for **3a**−**y** derivatives, presumably via possible inhibition of hemozoin crystal growth. However, the detailed study of the mechanisms of action underpinning high potency and improved selectivity of cryptolepine analogues will be a subject of the separate investigations.

Overall, cryptolepine derivatives containing basic side chains have been confirmed as promising lead compounds for the development of new, highly potent, and selective agents against the blood stages, but not the liver stage, of *P. falciparum* malaria.

Experimental Section

Chemistry. Chemicals were purchased from Sigma-Aldrich Chemical Co. Ltd., Spain and used without further purification All compounds were characterized through NMR spectroscopy and in some cases through mass spectrometry. NMR spectra were acquired on a Bruker 400 Ultrashield spectrometer at 400 MHz (^{1}H NMR) and 100 MHz (^{13}C NMR), using the solvent as internal reference. Coupling constants (*J*) are given in hertz. Mass spectra were recorded using a Micromass Autospec spectrometer with electronic impact as ionization method and high resolution mass spectra (accurate mass) were recorded on a Bruker Microtof spectrometer with ESI-TOF as ionization method (University of Santiago de Compostela, Spain). The purity of compounds submitted for biological testing were in all cases ≥95% as determined from elemental analysis (Supporting Information). C, H, and N analyses were carried out by the Unit Elemental Analysis, University of Santiago de Compostela, Spain, on a LECO model CHNS-932 elemental analyzer. UV−visible spectra for hematin binding studies were recorded on a Shimadzu UV-1603 UV−visible spectrometer with a temperature-controlled (25 °C) cell holder. Purified 12-mer double-stranded oligonucleotide $d(GATCCTAGGATC)_2$ was purchased from Atdbio, School of Chemistry, University of Southampton, UK. UV−visible spectral scans and absorbance readings for DNA binding studies were conducted using 1 cm path length quartz cuvettes in a Cary 4000 (Varian) UV−visible spectrophotometer equipped with a Peltier-thermostatted cuvette holder. Fluorescence emission and excitation spectra were recorded in 1 cm path length quartz cuvettes using a Cary-Eclipse (Varian) fluorescence spectrophotometer. Melting points were determined using a Bock-Monoscop M apparatus and are uncorrected. Reactions were monitored by thin-layer chromatography (TLC) using coated silica gel plates (Merck, aluminum sheets, silica gel 60 F_{254}).

General Procedure A. Preparation of 2-(2-Bromoacetamido)-benzoic Acid (5a). A solution of 2-amino-benzoic acid (10.0 g, 72.9 mmol) in DMF (30 mL) and 1,4-dioxane (30 mL) was cooled to 0 °C. Bromoacetyl bromide (8.0 mL, 91.7 mmol) was added dropwise over a 20 min period, keeping the internal

temperature between 0 and 1 °C. After the addition was complete, the ice bath was removed and stirring was continued overnight at room temperature. The reaction mixture was added to water (300 mL), and the light-yellow precipitate was filtered, washed with water until neutral pH, and then dried to give 18.1 g (96%) of **5a** as a white solid, mp 162−165 °C. ^{1}H NMR (400 MHz, CD_3OD) δ_H (ppm) 8.59 (d, J = 8.5 Hz, 1H), 8.13 (d, J = 8.0 Hz, 1H), 7.60 (dd, J = 8.5, 7.1 Hz, 1H), 7.21 (dd, J = 8.0, 7.1, Hz, 1H), 4.13 (s, 2H). ^{13}C NMR (100 MHz, CD_3OD) δ_C (ppm) 170.53, 166.71, 140.96, 134.61, 131.97, 124.02, 120.72, 117.33, 29.56.

2-(2-Bromoacetamido)-4-chlorobenzoic Acid (5b). Reaction of 2-amino-4-chloro benzoic acid (10 g, 58.2 mmol) and bromoacetyl bromide (6.3 mL, 72.8 mmol) according to general procedure A, gave 17.1 g (99%) of **5b** as a light-yellow solid, mp 166−168 °C. ^{1}H NMR (400 MHz, DMSO) δ_H (ppm) 11.73 (s, NH), 8.54 (d, J = 2.1 Hz, 1H), 7.98 (d, J = 8.6 Hz, 1H), 7.24 (dd, J = 8.6, 2.1 Hz, 1H), 4.28 (s, 2H). ^{13}C NMR (100 MHz, DMSO) δ_C (ppm) 169.03, 165.92, 141.54, 138.95, 133.26, 123.73, 119.61, 115.91, 30.98.

General Procedure B. Preparation of 2-(2-(Phenylamino)-acetamido)benzoic Acid (6a). A solution of **5a** (15.0 g, 58.1 mmol) and aniline (19.0 mL, 208.3 mmol) in DMF (30 mL) was heated at 120 °C for 18 h. After cooling, the reaction mixture was poured into ice−water (500 mL), the pH adjusted to 10−11 with 5% KOH, and then extracted with dichloromethane (3 × 300 mL). The combined dichloromethane extracts were set aside, and the aqueous layer was acidified to pH 3 with a solution of 5% HBr. The precipitate was collected, washed with water, and then dried, yielding 11.0 g (70%) of **6a** as a white solid, mp 194−197 °C. ^{1}H NMR (400 MHz, CD_3OD) δ_H (ppm) 8.72 (d, J = 8.0 Hz, 1H), 8.04 (d, J = 7.6 Hz, 1H), 7.57 (dd, J = 8.0, 7.5 Hz, 1H), 7.15 (dd, J = 7.5, 7.6 Hz, 1H), 7.14 (dd, J = 7.5, 8.0 Hz, 2H), 6.69 (d, J = 7.5 Hz, 1H), 6.65 (d, J = 8.0 Hz, 2H), 3.91 (s, 2H). ^{13}C NMR (100 MHz, CD_3OD) δ_C (ppm): 171.95, 170.81, 148.72, 141.15, 134.30, 132.03, 129.45, 123.56, 120.79, 118.47, 116.89, 113.37, 49.95.

4-Chloro-2-(2-(phenylamino)acetamido)benzoic Acid (6b). Reaction of **5b** (15 g, 51.3 mmol) with aniline (16.3 mL, 179.6 mmol) according to general procedure B gave 14.9 g of **6b** (96%) as a white solid, mp 217−220 °C. ^{1}H NMR (400 MHz, DMSO) δ_H (ppm) 12.13 (s, NH), 8.83 (d, J = 2.2 Hz, 1H), 7.94 (d, J = 8.6 Hz, 1H), 7.21 (dd, J = 8.6, 2.2 Hz, 1H), 7.10 (dd, J = 8.0, 7.4 Hz, 2H), 6.63 (d, J = 7.4 Hz, 1H), 6.59 (d, J = 8.0 Hz, 2H), 3.86 (s, 2H). ^{13}C NMR (100 MHz, DMSO) δ_C (ppm) 171.96, 168.80, 148.46, 141.99, 139.03, 133.33, 129.45, 123.08, 119.16, 117.63, 115.16, 112.90, 49.36.

4-Chloro-2-(2-(3-chlorophenylamino)acetamido)benzoic Acid (6c). Reaction of **5b** (3.0 g, 10.2 mmol) and 3-chloroaniline (3.34 mL, 31.7 mmol) in DMF (10 mL) was heated at 90 °C for 72 h and treated according to general procedure B to give 3.0 g of **6c** (84%) as a white solid, mp 223−226 °C. ^{1}H NMR (400 MHz, DMSO) δ_H (ppm) 12.10 (s, NH), 8.80 (d, J = 2.2 Hz, 1H), 7.95 (d, J = 8.6 Hz, 1H), 7.20 (dd, J = 8.6, 2.2 Hz, 1H), 7.11 (dd, J = 8.0 Hz, 1H), 6.84 (s, NH), 6.55 (m, 2H), 6.54 (dd, J = 8.2, 1.4 Hz, 1H), 3.92 (d, J = 5.5 Hz, 2H). ^{13}C NMR (100 MHz, DMSO) δ_C (ppm) 171.29, 168.95, 149.99, 141.93, 139.03, 134.00, 133.34, 131.02, 123.13, 119.16, 117.04, 115.24, 112.41, 111.32, 48.80.

General Procedure C. Preparation of Indolo[3,2-*b*]quinolin-11-one (7a). A mixture of **6a** (6.0 g, 21.5 mmol) and polyphosphoric acid (PPA, 200 g) was heated with mechanical stirring at 130 °C for 2 h. The reaction mixture was poured into ice−water (500 mL), neutralized with saturated KOH solution, and then extracted with AcOEt (2 × 250 mL). The extract was washed with water and brine, dried with anhydrous Na_2SO_4, and then concentrated to give 3.47 g (67%) of impure **7a** as a light-brown solid, mp > 300 °C. ^{1}H NMR (400 MHz, DMSO) δ_H (ppm) 12.41 (s, NH), 11.64 (s, NH), 8.29 (d, J = 7.9 Hz, 1H), 8.13 (d, J = 7.8 Hz, 1H), 7.72 (d, J = 7.4 Hz, 1H), 7.69 (dd, J = 8.3, 7.4 Hz, 1H), 7.51 (d, J = 8.4 Hz, 1H), 7.49 (dd, J = 8.4, 7.7 Hz, 1H), 7.29 (dd, J = 8.3, 7.9 Hz, 1H), 7.20 (dd, J = 7.7, 7.8 Hz, 1H). ^{13}C NMR (100 MHz, DMSO) δ_C (ppm) 167.77, 139.54, 139.05, 130.99, 129.44, 127.84, 125.57, 123.48, 123.24, 121.63, 120.87, 119.25, 118.28, 116.38, 112.98.

3-Chloro-indolo[3,2-*b*]quinolin-11-one (7b). A mixture of **6b** (2.0 g, 6.6 mmol) and PPA (60 g) was treated according to general procedure C, giving 0.630 g (36%) of **7b** as a light-green solid, mp > 300 °C. ^{1}H NMR (400 MHz, DMSO) δ_H (ppm) 12.56 (NH, 1H), 11.81 (NH, 1H), 8.35 (d, J = 8.7 Hz, 1H), 8.15 (d, J = 8.1 Hz, 1H), 7.73 (d, J = 1.8 Hz, 1H), 7.5 (d, J = 6.2 Hz, 1H), 7.49 (dd, J = 7.3, 6.2 Hz 1H), 7.30 (dd, J = 8.7, 1.8 Hz, 1H), 7.23 (dd, J = 8.1, 7.3 Hz, 1H). ^{13}C NMR (100 MHz, DMSO) δ_C (ppm) 167.30, 140.02, 139.08, 135.65, 129.40, 128.10, 127.94, 123.64, 121.96, 121.31, 121.15, 119.62, 117.13, 116.14, 113.17.

3,8-Dichloro-indolo[3,2-*b*]quinolin-11-one (7c). Compound **6c** (2.0 g, 5.90 mmol) reacted with PPA (60 g) according to general procedure C. After the extraction, the solvent was removed at reduced pressure and the residue purified by flash chromatography (silica gel 230−400 mesh, 40−63 μm, AcOEt:hexane, 6:4) to give 0.271 g (15%) of **7c** as light-green solid, mp > 300 °C. ^{1}H NMR (400 MHz, DMSO) δ_H (ppm) 12.27 (s, NH), 11.33 (s, NH), 8.36 (d, J = 2.0 Hz, 1H), 8.34 (d, J = 8.8 Hz, 1H), 7.49 (d, J = 0.9 Hz, 1H), 7.46 (d, J = 7.1 Hz, 1H), 7.33 (dd, J = 8.8, 2.0 Hz, 1H), 7.24 (dd, J = 7.1, 0.9 Hz, 1H). ^{13}C NMR (100 MHz, DMSO) δ_c (ppm) 167.49, 140.50, 139.88, 135.94, 128.69, 127.60, 127.45, 126.41, 124.33, 121.87, 121.73, 119.76, 118.64, 113.84, 112.24.

General Procedure D. Preparation of 11-Chloro-10*H*-indolo-[3,2-*b*]quinoline (8a). A solution of **7a** (1.5 g, 6.58 mmol) in $POCl_3$ (20 mL) was refluxed for 2 h. The reaction mixture was cooled, poured into ice, and neutralized with a cold KOH solution. The aqueous solution was then extracted with AcOEt (3 × 200 mL), and then the combined organic phases were washed with water and brine, dried with anhydrous Na_2SO_4, and then concentrated to give 0.95 g (60%) of impure **8a**, as a light-brown solid, mp 180−185 °C. ^{1}H NMR (400 MHz, DMSO) δ_H (ppm) 11.82 (s, NH), 8.28 (d, J = 7.7 Hz, 1H), 8.21 (m, 2H), 7.69 (m, 2H), 7.61 (m, 2H), 7.27 (m, 1H). ^{13}C NMR (100 MHz, DMSO) δ_C (ppm) 145.22, 143.32, 142.99, 129.55, 129.28, 128.43, 126.01, 125.54, 122.79, 121.30, 120.87, 120.34, 119.40, 117.14, 111.23.

3,11-Dichloro-10*H*-indolo[3,2-*b*]quinoline (8b). According with general procedure D, **7b** (1.5 g, 4.42 mmol) was reacted with $POCl_3$ (20 mL) to give 1.0 g of **8b** (66%) as a light-orange solid, mp 171−176 °C. ^{1}H NMR (400 MHz, DMSO) δ_H (ppm) 11.98 (s, NH), 8.33 (d, J = 7.8 Hz, 1H), 8.29 (d, J = 2.1 Hz, 1H), 8.28 (d, J = 9.2 Hz, 1H), 7.73 (m, 1H), 7.68 (dd, J = 7.0, 1.1 Hz, 1H), 7.63 (d, J = 8.1 Hz, 1H), 7.35 (dd, J = 7.8, 7.0 Hz, 1H). ^{13}C NMR (100 MHz, DMSO) δ_C (ppm) 147.43, 144.85, 144.34, 131.76, 131.27, 130.69, 128.07, 127.20, 124.66, 122.74, 122.35, 121.31, 120.89, 118.68, 112.64.

3,8,11-Trichloro-10*H*-indolo[3,2-*b*]quinoline (8c). Reaction of **7c** (0.25 g, 1.6 mmol) with $POCl_3$ (10 mL) according with general procedure D gave 0.13 g of **8c** (49%) as a strong orange solid, mp 167−170 °C. ^{1}H NMR (400 MHz, DMSO) δ_H (ppm) 12.14 (s, NH), 8.34 (d, J = 8.4 Hz, 1H), 8.31 (d, J = 1.9 Hz, 1H), 8.30 (d, J = 4.9 Hz, 1H), 7.77 (dd, J = 9.1, 2.0 Hz, 1H), 7.62 (s, 1H), 7.37 (dd, J = 8.3, 1.7 Hz, 1H). ^{13}C NMR (100 MHz, DMSO) δ_C (ppm) 146.48, 145.34, 144.56, 135.68, 132.23, 130.99, 128.04, 127.57, 124.82, 123.84, 122.82, 121.28, 120.19, 119.36, 112.29.

10*H*-Indolo[3,2-*b*]quinoline (9). To a portion of **8a** (0.27 g, 1.07 mmol), sodium acetate (1.1 g, 13.4 mmol), and 10% Pd/C in acetic acid (25 mL) was hydrogenated at 60 psi for 2 h. The reaction mixture was filtered to remove the catalyst, the solvent evaporated to a small volume and basified with ice-cold saturated solution of $NaHCO_3$, and then extracted with AcOEt (3 × 25 mL). The combined organic extracts were washed with water and brine, dried (anhydrous Na_2SO_4), and the solvent removed under reduced pressure to give 0.199 g (85%) of pure **9**, as a yellow solid, mp 200−203 °C. ^{1}H NMR (400 MHz, DMSO) δ_H (ppm) 11.43 (s, NH), 8.36 (d, J = 7.7 Hz, 1H), 8.29

(s, 1H), 8.20 (d, J = 8.5 Hz, 1H), 8.11 (d, J = 8.1 Hz, 1H), 7.61 (m, 4H), 7.29 (dd, J = 7.8, 7.0, 1H). ^{13}C NMR (100 MHz, DMSO) δ_C (ppm) 145.04, 143.34, 142.71, 131.75, 128.98, 128.01, 126.80, 126.03, 125.32, 124.15, 120.67, 120.29, 118.63, 112.31, 110.81.

5-Methyl-10*H*-indolo[3,2-*b*]quinolin-5-ium Trifluoro Methanesulfonate (1). A suspension of **9** (0.085 mg, 0.38 mmol) in anhydrous toluene (2 mL) was treated with methyl triflate (70 μL, 0.638 mmol), and the mixture was stirred at room temperature for 24 h. Diethyl ether was added (5 mL), and the resulting orange precipitate was filtered, washed with diethyl ether, and dried to give 0.092 g (62%) of pure **1**, mp > 300 °C. ^{1}H NMR (400 MHz, DMSO) δ_H (ppm) 12.75 (s, NH), 9.15 (s, 1H), 8.68 (d, J = 7.7 Hz, 1H), 8.65 (d, J = 8.5 Hz, 1H), 8.45 (d, J = 7.4 Hz, 1H), 8.06 (dd, J = 8.5, 6.4 Hz, 1H), 7.84 (m, 2H), 7.72 (d, J = 8.0 Hz, 1H), 7.42 (dd, J = 8.2, 7.7 Hz, 1H), 4.92 (s, 3H). ^{13}C NMR (100 MHz, DMSO) δ_C (ppm) 144.73, 137.06, 134.34, 132.97, 132.27, 131.44, 128.85, 126.09, 125.29, 125.24, 123.85, 120.41, 116.84, 112.86, 112.20, 39.21.

General Procedure E. Preparation of 5-Methyl-11-chloro-10*H*-indolo[3,2-*b*]quinolin-5-ium Chloride (10a). To a suspension of **8a** (2.0 g, 7.91 mmol) in anhydrous toluene (50 mL) was added methyl triflate (2.55 mL, 23.7 mmol), and the mixture stirred at room temperature for 48 h. The solid was filtered, suspended in sodium carbonate 5% (400 mL), and extracted with chloroform (3 × 400 mL). The chloroform extracts were washed with water and brine, dried (anhydrous Na_2SO_4), and concentrated to a small volume. The solution was acidified with HCl in diethyl ether to give, after filtration and drying, 2.15 g (90%) of pure **10a**, as an orange solid, mp 269−272 °C. ^{1}H NMR (400 MHz, DMSO) δ_H (ppm) 13.39 (s, NH), 8.88 (d, J = 9.4 Hz, 1H), 8.85 (d, J = 8.9 Hz, 1H), 8.69 (d, J = 8.3 Hz, 1H), 8.30 (dd, J = 9.4, 7.7 Hz, 1H), 8.12 (dd, J = 8.3, 7.7 Hz, 1H), 8.01 (dd, J = 8.4, 7.7 Hz, 1H), 7.90 (d, J = 8.4 Hz, 1H), 7.58 (dd, J = 8.9, 7.7 Hz, 1H), 5.04 (s, 3H). ^{13}C NMR (100 MHz, DMSO) δ_C (ppm) 146.33, 139.03, 136.15, 134.90, 133.20, 132.11, 129.30, 128.79, 126.98, 124.97, 123.73, 122.45, 119.21, 114.78, 113.94, 40.97.

5-Methyl-3,11-dichloro-10*H*-indolo[3,2-*b*]quinolin-5-ium Chloride (10b). A suspension of **8b** (0.15 g, 0.52 mmol) was treated with methyl triflate (114 μL, 1.04 mmol) according to general procedure E, giving 0.139 g of **10b** (79%) as an orange solid, mp 234−237 °C. ^{1}H NMR (400 MHz, DMSO) δ_H (ppm) 13.63 (NH, 1H), 9.00 (d, J = 1.7 Hz, 1H), 8.80 (d, J = 8.5 Hz, 1H), 8.60 (d, J = 9.1 Hz, 1H), 8.09 (dd, J = 9.1, 1.7 Hz, 1H), 7.96 (dd, J = 8.5, 7.4 Hz, 1H), 7.87 (d, J = 8.5 Hz, 1H), 7.53 (dd, J = 8.5, 7.4 Hz, 1H), 4.98 (s, 3H). ^{13}C NMR (100 MHz, DMSO) δ_C (ppm) 146.60, 139.54, 138.36, 136.52, 135.29, 132.30, 129.40, 129.34, 127.10, 126.98, 122.67, 122.52, 118.68, 114.73, 114.06, 41.27.

5-Methyl-3,8,11-trichloro-10*H*-indolo[3,2-*b*]quinolin-5-ium Chloride (10c). A suspension of **8c** (50 mg, 0.16 mmol) was treated with methyl triflate (35 μL, 0.32 mmol) according to general procedure E, giving 26.1 mg of **10c** (46%) as an orange solid, mp 229−233 °C. ^{1}H NMR (400 MHz, DMSO) δ_H (ppm) 13.47 (s, NH), 9.00 (s, 1H), 8.82 (d, J = 9.0 Hz, 1H), 8.62 (d, J = 9.1 Hz, 1H), 8.12 (d, J = 9.1 Hz, 1H), 7.81 (d, J = 1.5 Hz, 1H), 7.57 (dd, J = 9.0, 1.5 Hz, 1H), 4.95 (s, 3H). ^{13}C NMR (100 MHz, DMSO) δ_C (ppm) 146.69, 140.11, 139.05, 138.83, 136.77, 132.64, 129.97, 129.63, 128.70, 127.06, 123.19, 122.77, 118.73, 113.73, 113.41, 41.26.

General Procedure F. Preparation of 5-Methyl-11-(2-aminoethylamino)-10*H*-indolo[3,2-*b*]quinolin-5-ium Chloride (3a). To a suspension of **10a** (40 mg, 0,132 mmol) in AcOEt (5 mL) was added ethane-1,2-diamine (17.7 μL, 0.263 mmol) The reaction mixture was refluxed for 24 h, and the resulting precipitate collected, washed with dry diethyl ether, and evaporated. The solid was suspended in 5% sodium carbonate (20 mL) and extracted with chloroform (3 × 20 mL). The combined organic extracts were washed with water, dried with brine (20 mL) and anhydrous Na_2SO_4, and dried under reduced pressure. Recrystallization from chloroform with HCl in diethyl ether gave 61% (26.3 mg) of pure **3a**, as a light-yellow solid, mp 293−295 °C. ^{1}H NMR (400 MHz, DMSO) δ_H (ppm) 12.29 (s, NH) 9.24 (s, NH), 8.84 (d, J = 8.2 Hz, 1H), 8.51 (d, J = 8.4 Hz, 1H), 8.44 (s, NH_2), 8.31 (d, J = 8.8 Hz, 1H), 8.01 (d, J = 8.3 Hz, 1H), 7.97 (dd, J = 8.8, 7.4 Hz, 1H), 7.68 (dd, J = 8.3, 7.6 Hz, 1H), 7.64 (dd, J = 8.2, 7.4 Hz, 1H), 7.32 (d, J = 8.4, 7.6 Hz, 1H), 4.58 (s, 3H), 4.44 (m, 2H), 3.32 (m, 2H). ^{13}C NMR (100 MHz, DMSO) δ_C (ppm) 143.46, 142.90, 137.02, 132.27, 130.52, 126.72, 124.63, 124.29, 123.88, 120.75, 117.24, 115.95, 115.31, 114.32, 113.72, 42.41, 38,85, 38.08.

5-Methyl-11-[2-(Dimethylamino)ethylamino]-10*H*-indolo [3,2-*b*]-quinolin-5-ium Chloride (3b). To a suspension of **10a** (40.0 mg, 0.132 mmol) in AcOEt (5 mL) was added commercial N^1,N^1-dimethylethane-1,2-diamine (29 μL, 0.264 mmol). The reaction mixture was refluxed for 24 h, and the resulting precipitate was collected, washed with diethyl ether, and dried. The product was recrystallized from methanol−AcOEt to give 62% (29.2 mg) yield of pure **3b**, as a dark-yellow solid, mp 260−262 °C. ^{1}H NMR (400 MHz, CD_3OD) δ_H (ppm) 8.71 (d, J = 8.4 Hz, 1H), 8.48 (d, J = 8.2 Hz, 1H), 8.28 (d, J = 8.1 Hz, 1H), 8.03 (dd, J = 8.1, 7.6 Hz, 1H), 7.91 (d, J = 8.2 Hz, 1H), 7.73 (dd, J = 8.4, 7.6 Hz, 1H), 7.69 (dd, J = 8.2, 7.5 Hz, 1H), 7.40 (dd, J = 8.2, 7.5 Hz, 1H), 4.64 (s, 3H), 4.61 (t, J = 6.2 Hz, 2H), 3.72 (t, J = 6.2 Hz, 2H), 3.05 (s, 6H). ^{13}C NMR (100 MHz, CD_3OD) δ_C (ppm) 143.73, 143.16, 137.37, 136.93, 132.41, 131.06, 124.51, 123.78, 123.65, 121.19, 116.85, 116.74, 115.78, 114.67, 113.35, 56.55, 42.68, 40.51, 37.51.

5-Methyl-11-[2-(diethylamino)ethylamino]-10*H*-indolo[3,2-*b*]-quinolin-5-ium Chloride (3c). After recrystallization from methanol with ethyl acetate, the compound **3c** was obtained in 35% yield (18.4 mg) as a dark-yellow solid, mp > 330 °C, from **10a** (40.0 mg, 0.132 mmol) and commercially available N^1,N^1-diethylethane-1,2-diamine (37.1 μL, 0.264 mmol) according to general procedure F. ^{1}H NMR (400 MHz, CD_3OD) δ_H (ppm) 8.82 (d, J = 8.4 Hz, 1H), 8.53 (d, J = 8.1 Hz, 1H), 8.30 (d, J = 8.2 Hz, 1H), 7.98 (dd, J = 8.2, 7.7 Hz, 1H), 7.77 (d, J = 8.6 Hz, 1H), 7.70 (dd, J = 8.6, 7.2 Hz, 1H), 7.66 (dd, J = 8.2, 7.7 Hz, 1H), 7.34 (dd, J = 8.1, 7.2 Hz, 1H), 4.57 (s, 3H), 4.14 (s, 2H), 2.98 (s, 2H), 2.71 (q, J = 7.0 Hz, 4H), 0.95 (t, J = 7.0 Hz, 6H). ^{13}C NMR (100 MHz, CD_3OD) δ_C (ppm) 144.50, 143.39, 137.53, 135.48, 132.52, 130.71, 124.74, 124.51, 124.19, 120.83, 118.07, 117.68, 115.60, 115.55, 114.01, 53.41, 47.66, 44.62, 38.24, 11.27.

5-Methyl-11-[1-(dimethylamino)propan-2-ylamino]-10*H*-indolo-[3,2-*b*]quinolin-5-ium chloride (3d). This compound was obtained in 28% yield (13.9 mg) as an orange solid, mp 272−276 °C, by reaction of **10a** (40.0 mg. 0.132 mmol) and N^1,N^1-dimethylpropane-1,2-diamine **12** (26.6 mg, 0.264 mmol), according to general procedure F, and recrystallization from $CHCl_3$:MeOH (1:1) with AcOEt:Et_2O (3:2). ^{1}H NMR (400 MHz, DMSO+D_2O) δ_H (ppm) 8.69 (d, J = 8.5 Hz, 1H), 8.53 (d, J = 8.4 Hz, 1H), 8.30 (d, J = 8.9 Hz, 1H), 8.04 (dd, J = 7.1, 8.9 1H), 7.86 (d, J = 8.5 Hz, 1H), 7.77 (dd, J = 7.4, 8.5 Hz, 1H), 7.73 (d, J = 7.1, 8.5 Hz, 1H), 7.42 (dd, J = 7.4, 8.4 Hz 1H), 5.11 (m, 1H), 4.62 (s, 3H), 3.81 (t, J = 11.7 Hz 1H), 3.45 (d, J = 11.9 Hz 1H), 2.88 (s broad, 6H), 1.44 (d, J = 6.3 Hz, 3H). ^{13}C NMR (100 MHz, DMSO + D_2O) δ_C (ppm) 143.73, 143.11, 137.49, 135.73, 133.30, 132.04, 130.69, 125.17, 125.04, 124.82, 122.02, 117.76, 116.30, 115.01, 114.07, 60.90, 47.64, 44.03, 38.47, 20.56.

5-Methyl-11-(3-Aminopropylamino)-10*H*-indolo[3,2-*b*]quinolin-5-ium Chloride (3e). To a suspension of **10a** (40.0 mg, 0.132 mmol) was added commercial propane-1,3-diamine (22 μL, 0.264 mmol) according to general procedure F. The product was recrystallized from CH_2Cl_2:MeOH (8:2) with Et_2O to give 24.3 mg (54%) of **3e** as yellow solid, mp 243−245 °C. ^{1}H NMR (400 MHz, DMSO) δ_H (ppm) 12.28 (s, NH), 9.27 (s, NH), 8.90 (d, J = 8.6 Hz, 1H), 8.56 (d, J = 8.5 Hz, 1H), 8.36 (d, J = 8.9 Hz, 1H), 8.20 (s, NH_2), 8.03 (d, J = 8.0 Hz, 1H), 8.01 (dd, J = 8.9, 8.1 Hz, 1H), 7.73 (dd, J = 8.0, 7.6 Hz, 1H), 7.68 (dd, J = 8.6, 8.0 Hz, 1H), 7.37 (dd, J = 8.5, 7.6 Hz, 1H), 4.61 (s, 3H), 4.32 (d, J = 6.0 Hz, 2H), 3.01 (d, J = 5.7 Hz, 2H), 2.17 (dd, J = 6.0, 5.7 Hz, 2H). ^{13}C NMR (100 MHz,

DMSO) δ_C (ppm) 144.01, 143.21, 137.65, 135.83, 132.76, 130.88, 124.89, 124.74, 124.39, 121.17, 117.83, 116.59, 115.68, 114.75, 114.18, 42.86, 38.51, 36.75, 28.05.

5-Methyl-11-[3-(dimethylamino)propylamino]-10*H*-indolo [3,2-*b*]-quinolin-5-ium Chloride (3f). After recrystallization from methanol−ethyl acetate, **3f** was obtained in 34% yield (16.3 mg) as a dark-yellow solid, mp 277−280 °C, from **10a** (40.0 mg, 0.132 mmol) and commercial N^1,N^1-dimethylpropane-1,3-diamine (33.2 μL, 0.264 mmol), according to general procedure F. ^{1}H NMR (400 MHz, CD_3OD) δ_H (ppm) 8.65 (d, J = 8.4 Hz, 1H), 8.53 (d, J = 8.1 Hz, 1H), 8.30 (d, J = 8.1 Hz, 1H), 8.05 (dd, J = 8.1, 7.0 Hz, 1H), 7.92 (d, J = 8.1 Hz, 1H), 7.77 (d, J = 8.1, 7.1 Hz, 1H), 7.73 (dd, J = 8.4, 7.0 Hz, 1H), 7.44 (dd, J = 8.1, 7.1 Hz, 1H), 4.67 (s, 3H), 4.32 (t, J = 6.9 Hz, 2H), 3.37 (t, J = 7.9 Hz, 2H), 2.39 (quintet, J = 7.5 Hz, 2H), 2.92 (s, 6H). ^{13}C NMR (100 MHz, CD_3OD) δ_C (ppm) 143.63, 143.34, 137.46, 136.45, 134.47, 132.22, 130.71, 124.22, 123.62, 123.23, 120.93, 116.63, 115.51, 114.63, 113.13, 54.79, 42.50, 42.08, 37.22, 25.09.

5-Methyl-11-[3-(diethylamino)propylamino]-10*H*-indolo [3,2-*b*]-quinolin-5-ium Chloride (3g). The title compound was obtained in 82% yield (43.1 mg) as a dark-yellow solid, mp 274−277 °C, by reaction of **10a** (40.0 mg, 0.132 mmol) and commercially available N^1,N^1-diethylpropane-1,3-diamine (41.6 μL, 0.264 mmol), according to general procedure F. ^{1}H NMR (400 MHz, CD_3OD) δ_H (ppm) 8.62 (d, J = 8.5 Hz, 1H), 8.47 (d, J = 8.1 Hz, 1H), 8.25 (d, J = 8.5 Hz, 1H), 8.04 (dd, J = 8.5, 7.4 Hz, 1H), 7.91 (d, J = 8.4 Hz, 1H), 7.74−7.70 (m, 2H), 7.41 (dd, J = 8.1, 7.7 Hz, 1H), 4.59 (s, 3H), 4.29 (t, J = 7.0 Hz, 2H), 3.38 (t, J = 7.8 Hz, 2H), 3.26 (q, J = 7.2 Hz, 4H), 2.36 (quintet, J = 7.5 Hz, 2H), 1.34 (t, J = 7.2 Hz, 6H). ^{13}C NMR (100 MHz, CD_3OD) δ_C (ppm) 143.57, 143.36, 137.46, 136.35, 132.37, 130.81, 124.35, 123.68, 123.39, 121.08, 116.70, 116.53, 115.52, 114.63, 113.27, 49.08, 47.27, 42.84, 37.33, 24.65, 7.87.

5-Methyl-11-[3-(dimethylamino)-2,2-dimethylpropyl amino]-10*H*-indolo[3,2-*b*]quinolin-5-ium Chloride (3h). Reaction of **10a** (51.2 mg, 0.164 mmol) and commercial N^1,N^1-2,2-tetramethyl-propane-1,3-diamine (0.26 mL, 1.64 mmol), according to general procedure F, gave **3h** in 78% yield (52.6 mg), as an orange solid, mp 171−173 °C. ^{1}H NMR (400 MHz, DMSO) δ_H (ppm) 10.75 (s, NH), 8.51 (d, J = 8.1 Hz, 1H), 8.33 (d, J = 8.5 Hz, 1H), 8.20 (d, J = 7.9 Hz, 1H), 8.00 (dd, J = 8.5, 7.5 Hz, 1H), 7.93 (d, J = 8.1 Hz, 1H), 7.75 (dd, J = 7.9, 7.5 Hz, 1H), 7.67 (dd, J = 8.1, 7.6 Hz, 1H), 7.32 (dd, J = 8.1, 7.6 Hz, 1H), 4.56 (s, 3H), 4.21 (s, 2H), 2.59 (s, 2H), 2.44 (s, 6H), 1.13 (s, 6H). ^{13}C NMR (100 MHz, DMSO) δ_C (ppm) 144.59, 143.08, 137.67, 135.60, 132.62, 130.61, 124.83, 124.56, 123.11, 120.99, 118.02, 116.63, 115.58, 114.88, 114.18, 70.03, 57.33, 48.18, 38.31, 35.51, 25.38.

5-Methyl-11-[3-(isopropylamino)propylamino]-10*H*-indolo[3,2-*b*]-quinolin-5-ium Chloride (3i). After recrystallization from methanol−ethyl acetate, **3i** was obtained in 56% yield (28.7 mg) as a yellow solid, mp >330 °C, from reaction of **10a** (40.0 mg, 0.132 mmol) with commercial N^1-isopropylpropane-1,3-diamine (36.9 μL, 0.264 mmol) according to general procedure F. ^{1}H NMR (400 MHz, CD_3OD) δ_H (ppm) 8.67 (d, J = 8.3 Hz, 1H), 8.54 (d, J = 8.2 Hz, 1H), 8.30 (d, J = 8.4 Hz, 1H), 8.05 (dd, J = 8.4, 7.3 Hz, 1H), 7.93 (d, J = 8.1 Hz, 1H), 7.75 (dd, J = 8.1, 7.2 Hz, 1H), 7.73 (dd, J = 8.3, 7.3 Hz, 1H), 7.44 (dd, J = 8.2, 7.2 Hz, 1H), 4.68 (s, 3H), 4.34 (t, J = 7.0 Hz, 2H), 3.42 (quintet, J = 6.5 Hz, 1H), 3.27 (t, J = 7.6 Hz, 2H), 2.43 (quintet, J = 7.3 Hz, 2H), 1.37 (d, J = 6.5 Hz, 6H). ^{13}C NMR (100 MHz, CD_3OD) δ_C (ppm) 143.86, 143.76, 137.68, 135.73, 132.43, 130.92, 124.43, 123.82, 123.43, 121.16, 116.85, 115.72, 114.79, 113.30, 50.86, 42.65, 42.22, 37.43, 26.93, 17.91.

5-Methyl-11-[3-(piperidin-1-yl)propylamino]-10*H*-indolo [3,2-*b*]-quinolin-5-ium Chloride (3j). The title compound was obtained in 71% yield (38.3 mg) as a light-orange solid, mp 289−293 °C, after reaction of **10a** (40.0 mg, 0.132 mmol) with 3-piperidine-1yl-propan-1-amine **15** (37.5 mg, 0.264 mmol), according to general procedure F, and recrystallization from $CHCl_3$:MeOH (5:1) with AcOEt:Et_2O (8:1). ^{1}H NMR (400 MHz, DMSO) δ_H (ppm) 12.31 (s, NH), 9.21 (s, NH), 8.87 (d, J = 8.1 Hz, 1H), 8.55 (d, J = 8.1 Hz, 1H), 8.34 (d, J = 8.9 Hz, 1H), 8.01 (m, 2H), 7.71 (dd, J = 7.5, 6.5 Hz, 1H), 7.68 (dd, J = 8.1, 4.9 Hz, 1H), 7.36 (dd, J = 8.1, 6.5 Hz, 1H), 4.60 (s, 3H), 4.31 (m, J = 5.5 Hz, 2H), 3.43 (m, 2H), 3.23 (m, 2H), 2.86 (m, 2H), 2.30 (m, 2H), 1.78 (m, 4H), 1.69 (m, 1H), 1.38 (m, 1H). ^{13}C NMR (100 MHz, DMSO) δ_C (ppm) 143.41, 142.61, 137.02, 135.16, 132.12, 130.20, 124.44, 124.09, 123.70, 120.52, 117.15, 116.06, 115.02, 114.17, 113.58, 53.24, 51.81, 42.93, 37.89, 23.86, 22.12, 21.28.

5-Methyl-11-[4-aminobutylamino]-10*H*-indolo[3,2-*b*]quinolin-5-ium Chloride (3k). To a suspension of **10a** (40.0 mg, 0.132 mmol) was added commercial butane-1,4-diamine (26.6 μL, 0.264 mmol) according to general procedure F. The product was recrystallized from CH_2Cl_2:MeOH (7:3) with Et_2O to give 21.2 mg (45%) of **3k** as a yellow solid, mp 263−265 °C. ^{1}H NMR (400 MHz, DMSO) δ_H (ppm) 8.89 (d, J = 8.5 Hz, 1H), 8.55 (d, J = 8.2 Hz, 1H), 8.34 (d, J = 8.5 Hz, 1H), 8.00 (dd, J = 8.3, 7.3 Hz, 1H), 7.95 (d, J = 8.3 Hz, 1H), 7.71 (dd, J = 7.8, 7.3 Hz, 1H), 7.67 (dd, J = 8.3, 7.3 Hz, 1H), 7.36 (dd, J = 8.2, 7.3 Hz, 1H), 4.60 (s, 3H), 4.22 (t, J = 6.6 Hz, 2H), 2.85 (t, J = 7.4 Hz, 2H), 1.89 (m, 2H), 1.75 (m, 2H). ^{13}C NMR (100 MHz, DMSO) δ_C (ppm) 144.20, 143.13, 143.08, 137.77, 137.73, 132.70, 130.77, 125.01, 124.69, 124.26, 121.12, 117.78, 115.67, 114.93, 114.18, 45.18, 38.78, 38.45, 27.12, 24.75.

5-Methyl-11-[4-(diethylamino)butylamino]-10*H*-indolo [3,2-*b*]-quinolin-5-ium chloride (3l). The title compound was obtained in 70% yield (44.9 mg) as an orange solid, mp 268−272 °C, by reaction of **10a** (47.0 mg, 0.155 mmol) with N^1,N^1-diethylbutane-1,4-diamine **18** (44.8 mg, 0.31 mmol), according to general procedure F, and recrystallization from MeOH with AcOEt:Et_2O (2:3). ^{1}H NMR (400 MHz, DMSO) δ_H (ppm) 12.36 (s, NH), 9.24 (d, J = 1.3 Hz, NH), 8.89 (d, J = 8.1 Hz, 1H), 8.55 (d, J = 8.1 Hz, 1H), 8.33 (d, J = 8.6 Hz, 1H), 8.01 (dd, J = 8.6, 7.6 Hz, 1H), 7.98 (d, J = 8.1 Hz, 1H), 7.72 (dd, J = 8.1, 7.6 Hz, 1H), 7.68 (dd, J = 8.1, 7.6 Hz, 1H), 7.38 (dd, J = 8.1, 7.6 Hz, 1H), 4.60 (s, 3H), 4.23 (q broad, 2H), 3.10 (m, 6H), 1.89 (m, 4H), 1.21 (t, J = 7.1 Hz, 6H). ^{13}C NMR (100 MHz, DMSO) δ_C (ppm) 143.75, 142.58, 137.38, 135.13, 132.78, 132.23, 130.28, 124.58, 124.18, 123.76, 120.63, 117.26, 115.16, 114.40, 113.67, 50.27, 45.97, 44.76, 37.95, 26.82, 20.51, 8.34.

5-Methyl-11-[5-(diethylamino)pentan-2-ylamino]-10*H*-indolo-[3,2-*b*]quinolin-5-ium Chloride (3m). Reaction of **10a** (40.0 mg, 0.132 mmol) and N^1,N^1-diethylpentane-1,4-diamine (51 μL, 0.264 mmol), according to general procedure F, and recrystallization from MeOH with AcOEt:Et_2O (1:1), gave **3m** in 30% yield (17.2 mg), as an orange solid, mp 240−243 °C. ^{1}H NMR (400 MHz, DMSO) δ_H (ppm) 8.85 (d, J = 8.6 Hz, 1H), 8.58 (d, J = 8.1 Hz, 1H), 8.37 (d, J = 8.5 Hz, 1H), 8.04 (dd, J = 8.5, 7.8 Hz, 1H), 7.96 (d, J = 8.5 Hz, 1H), 7.76 (dd, J = 8.5, 7.7 Hz, 1H), 7.71 (dd, J = 8.6, 7.8 Hz, 1H), 7.39 (dd, J = 8.1, 7.7 Hz, 1H), 4.92 (m, 1H), 4.64 (s, 3H), 3.13−2.93 (m, 6H), 2.14−1.98 (m, 2H), 1.91−1.81 (m, 2H), 1.47 (d, J = 6.2 Hz, 3H), 1.14 (t, J = 7.1 Hz, 6H). ^{13}C NMR (100 MHz, DMSO) δ_C (ppm) 144.24, 143.36, 140.38, 138.04, 136.08, 132.93, 131.09, 125.73, 124.98, 124.46, 121.39, 118.04, 116.04, 115.25, 114.41, 51.01, 46.88, 46.69, 38.87, 34.15, 22.55, 20.75, 9.01.

5-Methyl-11-(piperidin-4-ylamino)-10*H*-indolo[3,2-*b*]quinolin-5-ium Chloride (3n). Reaction of **10a** (50.0 mg, 0.165 mmol) and piperidin-4-amine (31.1 μL, 0.296 mmol), according to general procedure F, gave **3n** in 66% yield (40.3 mg), as an orange solid, mp 325−327 °C. ^{1}H NMR (400 MHz, DMSO) δ_H (ppm) 8.66 (d, J = 8.3 Hz, 1H), 8.56 (d, J = 8.6 Hz, 1H), 8.29 (d, J = 6.2 Hz, 1H), 8.09 (dd, J = 8.6, 5.6 Hz, 1H), 7.97 (d, J = 6.3 Hz, 1H), 7.84 (dd, J = 6.2, 5.6 Hz, 1H), 7.81 (dd, J = 6.3, 5.6 Hz, 1H) 7.44 (dd, J = 8.3, 5.6 Hz, 1H), 4.80 (s, 3H), 4.14 (d, J = 12.8 Hz, 2H), 3.85 (t, J = 11.6 Hz, 2H), 3.50 (m, 1H), 2.28 (t, J = 11.6 Hz, 2H), 2.10−1.97 (m, 2H). ^{13}C NMR (100 MHz, DMSO) δ_C (ppm) 147.18, 144.35, 138.14, 137.77, 132.73, 132.51, 126.54, 125.71, 125.57, 125.00, 121.64, 120.67, 118.66, 114.74, 114.12, 51.16, 47.64, 39.63, 30.70.

5-Methyl-11-(1-isobutylpiperidin-4-ylamino)-10*H*-indolo[3,2-*b*]-quinolin-5-ium Chloride (3o). To a solution of **3n** (40.0 mg,

0.108 mmol), anhydrous Na_2SO_4 (2 g) and isobutyraldehyde (31.2 μL, 0.432 mmol) in dry MeOH (5 mL) was added $NaBH_3CN$ (33.9 mg, 0.54 mmol) and the reaction allowed to proceed at room temperature for 24 h. The anhydrous Na_2SO_4 was filtered off and solvent removed under reduced pressure. The resulting residue was dissolved in water (5 mL) and basified with aqueous KOH 2 M to pH 12. The aqueous solution was then extracted with CH_2Cl_2 (3 × 20 mL) and the combined organic extracts washed with water and brine, dried (anhydrous Na_2SO_4), and concentrated to a small volume under reduced pressure. HCl in Et_2O was added, and the resultant precipitate was collected, washed with Et_2O, and dried, yielding 27.3 mg (59%) of **3o** as a orange solid, mp 270−274 °C. ^{1}H NMR (400 MHz, CD_3OD) δ_H (ppm) 8.64 (d, J = 8.2 Hz, 1H), 8.51 (d, J = 8.3 Hz, 1H), 8.46 (d, J = 8.2 Hz, 1H), 8.13 (dd, J = 8.3, 7.6 Hz, 1H), 7.94 (d, J = 8.4 Hz, 1H), 7.88 (dd, J = 8.2, 7.6 Hz, 1H), 7.84 (dd, J = 8.4, 7.3 Hz, 1H), 7.50 (dd, J = 8.2, 7.3 Hz, 1H), 4.90 (s, 3H), 4.27 (d, J = 12.6 Hz, 2H), 3.92 (t, J = 12.2 Hz, 2H), 3.70 (m, 1H), 3.09 (d, J = 7.2 Hz, 2H), 2.52 (d, J = 11.2 Hz, 2H), 2.26 (qd, J = 12.1, 3.6 Hz, 2H), 2.16 (m, 1H), 1.16 (d, J = 6.7 Hz, 6H). ^{13}C NMR (100 MHz, CD_3OD) δ_C (ppm) 148.15, 146.06, 139.80, 139.53, 133.83, 133.81, 127.47, 126.81, 126.74, 126.07, 122.92, 122.55, 118.88, 115.94, 114.71, 56.97, 53.37, 52.21, 39.89, 30.22, 27.66, 20.52.

5-Methyl-11-(1-benzylpiperidin-4-ylamino)-10*H*-indolo [3,2-*b*]-quinolin-5-ium Chloride (3p). To a solution of **3n** (40.0 mg, 0.108 mmol) and anhydrous Na_2SO_4 (2 g) in dry MeOH (5 mL) was added benzaldehyde (43.6 μL, 0.432 mmol) and the mixture stirred for 1 h. $NaBH_3CN$ (33.9 mg, 0.54 mmol) was added and the mixture left to react for a further 20 h. The anhydrous Na_2SO_4 was filtered off and the solvent removed under reduced pressure. The residue was dissolved in H_2O (5 mL) and the pH adjusted to 12 with 2 M KOH. The aqueous solution was extracted with CH_2Cl_2 (3 × 20 mL) and the combined extracts washed with water and brine and dried with anhydrous Na_2SO_4. After concentration under reduced pressure, HCl in Et_2O was added to precipitate the product as a salt, which was filtered and recrystallized with MeOH:AcOEt (2:5) and Et_2O to give **3p** as a deep-yellow solid, mp 275−277 °C, in 66% yield. ^{1}H NMR (400 MHz, DMSO) δ_H (ppm) 8.63 (d, J = 8.2 Hz, 1H), 8.50 (d, J = 8.5 Hz, 1H), 8.47 (d, J = 8.2 Hz, 1H), 8.12 (dd, J = 8.5, 7.6 Hz, 1H), 7.93 (d, J = 8.1 Hz, 1H), 7.87 (dd, J = 8.2, 7.6 Hz, 1H), 7.83 (dd, J = 8.1, 7.6 Hz, 1H), 7.66 (d, J = 5.9 Hz, 2H), 7.56 (d, J = 6.7 Hz, 1H), 7.52 (dd, J = 6.7, 5.9 Hz, 2H), 7.48 (dd, J = 8.2, 7.6 Hz, 1H), 4.88 (s, 3H), 4.44 (s, 2H), 4.27 (d, J = 12.5 Hz, 2H), 3.92 (t, J = 12.5 Hz, 2H), 3.77 (t, J = 10.3 Hz, 1H), 2.58 (d, J = 11.6 Hz, 2H), 2.28 (q, J = 11.6 Hz, 2H). ^{13}C NMR (100 MHz, DMSO) δ_C (ppm) 146.67, 144.61, 138.35, 138.06, 135.98, 132.38, 132.35, 131.28, 129.71, 129.37, 129.01, 126.03, 125.32, 124.61, 121.46, 121.12, 117.42, 114.47, 113.27, 54.92, 50.73, 48.32, 38.46, 28.93.

5-Methyl-11-[1-(2-hydroxybenzyl)piperidin-4-ylamino]-10*H*-indolo[3,2-*b*]quinolin-5-ium Chloride (3q). Reaction of **3n** (40.0 mg, 0.108 mmol) with salicylaldehyde (45 μL, 0.432 mmol) according to the procedure described for **3o**, gave **3q**, in 30% yield (15.8 mg), as an orange solid, mp 277−280 °C. ^{1}H NMR (400 MHz, DMSO) δ_H (ppm) 12.18 (s, NH), 9.47 (d, J = 1.2 Hz, NH), 8.67 (d, J = 8.1 Hz, 1H), 8.58 (d, J = 8.8 Hz, 1H), 8.30 (d, J = 8.3 Hz, 1H), 8.10 (dd, J = 8.8, 7.1 Hz, 1H), 7.99 (d, J = 8.6 Hz, 1H), 7.86 (dd, J = 8.3, 7.1 Hz, 1H), 7.82 (dd, J = 8.6, 7.3 Hz, 1H), 7.56 (d, J = 7.2 Hz, 1H), 7.46 (dd, J = 8.1, 7.3 Hz, 1H), 7.28 (dd, J = 7.8, 6.9 Hz, 1H), 7.04 (d, J = 7.8 Hz, 1H), 6.89 (dd, J = 7.2, 6.9 Hz, 1H), 4.82 (s, 3H), 4.23 (s, 2H), 4.17 (d, J = 12.2 Hz, 2H), 3.85 (t, J = 11.5 Hz, 2H), 3.53 (m, 1H), 2.46 (d broad, 2H), 2.23 (q, J = 5.8 Hz, 2H). ^{13}C NMR (100 MHz, DMSO) δ_C (ppm) 155.99, 146.54, 143.94, 137.56, 137.28, 132.21, 132.19, 131.95, 131.63, 130.34, 125.97, 125.04, 124.60, 121.15, 121.07, 119.04, 118.24, 118.13, 115.44, 114.19, 113.67, 53.78, 50.74, 42.04, 39.27, 28.39.

5-Methyl-11-(phenylamino)-10*H*-indolo[3,2-*b*]quinolin-5-ium Chloride (3r). Following general procedure F, a suspension of **10a** (40.0 mg, 0.132 mmol) was allowed to react with aniline (21.7 μL, 0.24 mmol) to give **3r** (75%), mp 269−271 °C, after recrystallization with MeOH:AcOEt (1:2) and Et_2O. ^{1}H NMR (400 MHz, DMSO) δ_H (ppm) 8.49 (d, J = 8.6 Hz, 1H), 8.44 (d, J = 8.5 Hz, 1H), 8.34 (d, J = 8.7 Hz, 1H), 8.03 (dd, J = 8.7, 7.6 Hz, 1H), 7.69 (dd, J = 8.6, 7.6 Hz, 1H), 7.65 (dd, J = 8.2, 7.6 Hz, 1H), 7.53 (d, J = 8.2 Hz, 1H), 7.41 (dd, J = 7.8, 7.5 Hz, 2H), 7.35 (dd, J = 8.5, 7.6 Hz, 1H), 7.28 (d, J = 7.5 Hz, 1H), 7.18 (d, J = 7.8 Hz, 2H), 4.65 (s, 3H). ^{13}C NMR (100 MHz, DMSO) δ_C (ppm) 143.26, 139.75, 138.78, 137.94, 137.48, 133.65, 132.87, 130.98, 130.51, 126.69, 126.09, 125.34, 125.04, 122.76, 122.32, 118.39, 118.18, 115.27, 114.22, 38.83.

5-Methyl-11-[4-(piperidin-1-yl)phenylamino]-10*H*-indolo [3,2-*b*]-quinolin-5-ium Chloride (3s). Reaction of 4-(piperidin-1-yl)-benzenamine (41.6 mg, 0.236 mmol) with **10a** (40 mg, 0.132 mmol), according with general procedure F, gave **3s** as a yellow solid, mp 311−312 °C in 66% yield, after recrystallization using MeOH:AcOEt (1:3) and Et_2O. ^{1}H NMR (400 MHz, DMSO) δ_H (ppm) 8.65 (d, J = 8.1 Hz, 1H), 8.57 (d, J = 8.1 Hz, 1H), 8.42 (d, J = 8.1 Hz, 1H), 8.10 (dd, J = 8.1, 7.7 Hz, 1H), 7.76 (dd, J = 8.1, 7.7 Hz, 1H), 7.71 (dd, J = 8.0, 7.6 Hz, 1H), 7.60 (d, J = 8.0 Hz, 1H), 7.43 (dd, J = 8.1, 7.6 Hz, 1H), 7.31 (d, J = 8.1 Hz, 2H), 7.16 (d, J = 8.1 Hz, 2H), 4.81 (s, 3H), 3.37 (s broad, 4H), 1.80 (s broad, 4H), 1.69 (d, J = 4.6 Hz, 2H). ^{13}C NMR (100 MHz, DMSO) δ_C (ppm) 152.10, 143.89, 141.13, 139.22, 137.94, 133.79, 132.58, 132.35, 129.48, 125.95, 125.87, 125.31, 125.21, 122.48, 118.32, 118.25, 116.21, 114.45, 113.30, 51.89, 39.01, 26.85, 25.23.

5-Methyl-11-{4-[(diethylamino)methyl]-3-hydroxyphenyl amino}-10*H*-indolo[3,2-*b*]quinolin-5-ium Chloride (3t). A solution of *N*-(4-((diethylamino)-methyl)-3-hydroxyphenyl)-acetamido **20** (47.2 mg, 0.199 mmol) and **10a** (40 mg, 0.132 mmol) in HCl 6 M (10 mL) was refluxed for 20 h. After this period, the solution was concentrated under reduced pressure and the residue dissolved in Na_2CO_3 5% (25 mL). The aqueous solution was extracted with CH_2Cl_2 (3 × 20 mL) and the combined fractions washed with water and then dried with NaCl (satd) and with anhydrous Na_2SO_4. After concentration under reduced pressure, HCl in Et_2O was added and the precipitate formed, filtered off, and dried to give **3t** as an orange solid, mp 228−231 °C, in 31% yield. ^{1}H NMR (400 MHz, DMSO) δ_H (ppm) 11.84 (s, 1H), 10.98 (s, 1H), 10.63 (s, 1H), 8.67 (d, J = 8.9 Hz, 1H), 8.60 (d, J = 8.5 Hz, 1H), 8.58 (d, J = 8.5 Hz, 1H), 8.09 (dd, J = 8.5, 7.0 Hz, 1H), 7.78 (dd, J = 8.2, 6.2 Hz, 1H), 7.76 (d, J = 8.2 Hz, 1H), 7.74 (dd, J = 8.5, 7.0 Hz, 1H), 7.46 (d, J = 8.3 Hz, 1H), 7.43 (dd, J = 8.9, 6.2 Hz, 1H), 6.95 (d, J = 2.0 Hz, 1H), 6.67 (dd, J = 8.3, 2.0 Hz, 1H), 4.83 (s, 3H), 4.20 (d, J = 4.8 Hz, 2H), 3.13 (m, 4H), 1.29 (t, J = 7.1 Hz, 6H). ^{13}C NMR (100 MHz, DMSO) δ_C (ppm) 157.28, 144.25, 142.71, 142.22, 137.68, 136.58, 136.19, 133.43, 132.91, 132.32, 125.61, 125.22, 124.93, 120.99, 118.48, 117.94, 114.94, 113.60, 113.36, 111.83, 107.90, 49.49, 46.05, 39.32, 8.50.

5-Methyl-11-(pyridin-3-ylamino)-10*H*-indolo[3,2-*b*]quinolin-5-ium Chloride (3u). To a solution of **10a** (40.0 mg, 0.132 mmol) in DMF (5 mL) was added pyridin-3-amine (37.2 mg, 0.396 mmol) and the mixture heated at 100 °C for 48 h. Solvent was removed under reduced pressure. The remaining crude mixture was dissolved in Na_2CO_3 5% (20 mL) and extracted with CH_2Cl_2 (3 × 30 mL). The combined organic extracts were washed with water and brine and dried with anhydrous Na_2SO_4. After concentration under reduced pressure, HCl in Et_2O was added and the formed precipitate was filtered, washed with Et_2O, and dried in a vacuum line, to give **3u** in 48% yield as a brown solid (22.6 mg), mp 157−159 °C. ^{1}H NMR (400 MHz, DMSO) δ_H (ppm) 11.64 (s, NH), 8.79 (d, J = 8.4 Hz, 1H), 8.69 (d, J = 8.4 Hz, 1H), 8.64 (s, 1H), 8.63 (d, J = 7.2 Hz, 1H), 8.46 (d, J = 8.2 Hz, 1H), 8.13 (dd, J = 8.2, 7.2 Hz, 1H), 7.82 (dd, J = 8.4, 7.2 Hz, 1H), 7.79 (dd, J = 7.8, 7.5 Hz, 1H), 7.67 (d, J = 7.8 Hz, 1H), 7.63 (d, J = 5.7 Hz, 1H), 7.51 (dd, J = 8.2, 5.7 Hz, 1H), 7.44 (dd, J = 8.4, 7.2 Hz, 1H), 4.86 (s, 3H). ^{13}C NMR (100 MHz, DMSO) δ_C (ppm) 143.65, 143.62, 141.60, 137.89,

137.44, 137.42, 132.83, 132.58, 128.32, 125.62, 125.53, 125.37, 124.77, 124.55, 121.95, 121.60, 118.69, 118.49, 115.16, 113.88, 49.05.

3-Chloro-5-methyl-11-[3-(diethylamino)propylamino]-10*H*-indolo[3,2-*b*]quinolin-5-ium Chloride (3v). To a suspension of **10b** (40.0 mg, 0.118 mmol) in AcOEt (5 mL) was added commercial N^1,N^1-diethylpropane-1,3-diamine (21.4 μL, 0.212 mmol), according to general procedure F, giving 25.1 mg (53%) of **3v**, as a dark-yellow solid, mp 231−234 °C. ^{1}H NMR (400 MHz, DMSO): δ_H (ppm) 12.49 (s, NH), 9.41 (s, NH), 8.91 (d, J = 9.1 Hz, 1H), 8.55 (d, J = 8.4 Hz, 1H), 8.46 (s, 1H), 8.00 (d, J = 8.2 Hz, 1H), 7.73 (d, J = 8.0 Hz, 1H), 7.72 (dd, J = 9.1, 7.4 Hz, 1H), 7.37 (dd, J = 8.4, 7.4 Hz, 1H), 4.59 (s, 3H), 4.32 (s broad, 2H), 3.30 (s broad, 3H), 3.11 (q broad, 2H), 2.26 (s broad, 2H), 1.22 (t, J = 6.7 Hz, 6H). ^{13}C NMR (100 MHz, DMSO) δ_C (ppm) 144.12, 143.29, 138.45, 137.87, 135.95, 131.01, 127.17, 124.71, 124.56, 121.35, 117.52, 117.24, 116.94, 114.79, 114.41, 48.56, 46.49, 43.60, 38.83, 24.39, 8.87.

3-Chloro-5-methyl-11-(piperidin-4-ylamino)-10*H*-indolo[3,2-*b*]-quinolin-5-ium Chloride (3w). To a suspension of **10b** (30.0 mg, 0.088 mmol) in AcOEt (5 mL) was added piperidin-4-amine (18.6 μL, 0.177 mmol), according to general procedure F, giving 18.8 mg (53%) of **3w**, as a dark-yellow solid, mp 320−322 °C. ^{1}H NMR (400 MHz, DMSO) δ_H (ppm) 12.37 (s, NH), 8.71 (s, 1H), 8.66 (d, J = 8.2 Hz, 1H), 8.63 (s, NH), 8.28 (d, J = 9.1 Hz, 1H), 8.03 (d, J = 8.0 Hz, 1H), 7.88 (d, J = 9.1 Hz, 1H), 7.82 (dd, J = 8.0, 7.7 Hz, 1H), 7.44 (dd, J = 8.2, 7.7 Hz, 1H), 4.79 (s, 3H), 4.18 (d, J = 11.6 Hz, 2H), 3.92 (t, J = 10.7 Hz, 2H), 3.54 (m, 1H), 2.33 (d, J = 11.6 Hz, 2H), 2.07 (q, J = 10.7 Hz, 2H). ^{13}C NMR (100 MHz, DMSO) δ_C (ppm) 147.35, 144.48, 138.78, 137.90, 137.69, 132.52, 128.75, 125.82, 125.59, 124.90, 121.76, 119.25, 118.00, 114.63, 114.33, 51.38, 47.54, 39.49, 30.72.

3,8-Dichloro-5-methyl-11-(piperidin-4-ylamino)-10*H*-indolo-[3,2-*b*]quinolin-5-ium Chloride (3x). To a suspension of **10c** (21.7 mg, 0.058 mmol) in AcOEt (5 mL) was added piperidin-4-amine (11.3 μL, 0.116 mmol), according to general procedure F, giving 7.7 mg (30%) of **3x** as an orange solid, mp 315−317 °C. ^{1}H NMR (400 MHz, CD_3OD) δ_H (ppm) 8.55 (d, J = 8.9 Hz, 1H), 8.53 (s, 1H), 8.35 (d, J = 9.1 Hz, 1H), 7.90 (s, 1H), 7.80 (d, J = 9.1 Hz, 1H), 7.41 (d, J = 8.9 Hz, 1H), 4.75 (s, 3H), 4.23 (d, J = 12.1 Hz, 2H), 3.91 (t, J = 12.1 Hz, 2H), 3.64 (s broad, 1H), 2.38 (d, J = 11.4 Hz, 2H), 2.15 (d, J = 11.4 Hz, 2H). ^{13}C NMR (100 MHz, DMSO) δ_C (ppm) 148.61, 145.94, 140.28, 140.16, 139.76, 139.18, 129.34, 127.27, 126.67, 124.91, 123.55, 120.84, 118.38, 114.47, 114.23, 52.29, 49.22, 39.93, 31.62.

5-Methyl-11-(diethylamino)-10*H*-indolo[3,2-*b*]quinolin-5-ium chloride (3y). To a solution of **10a** (40 mg, 0.132 mmol) in DMF (10 mL) was added diethylamine (54.8 μL, 0.528 mmol) and the mixture allowed to react overnight at room temperature. The solvent was removed at reduced pressure, and the solid was suspended in 5% sodium carbonate (20 mL) and extracted with chloroform (3 × 20 mL). The combined organic extracts were washed with water and brine (20 mL) and dried with anhydrous Na_2SO_4, and the solvent was removed under reduced pressure. Recrystallization from chloroform with HCl in diethyl ether gave 65% (29.3 mg) of pure **3y**, as a light-yellow solid, mp 251−254 °C. ^{1}H NMR (400 MHz, CD_3OD) δ_H (ppm) 8.54 (d, J = 8.5 Hz, 1H), 8.45 (d, J = 8.5 Hz, 1H), 8.41 (d, J = 9.0 Hz, 1H), 8.02 (dd, J = 9.0, 8.4 Hz, 1H), 7.81 (d, J = 8.4 Hz, 1H), 7.75 (dd, J = 8.5, 8.4 Hz, 1H), 7.71 (dd, J = 8.4, 7.7 Hz, 1H), 7.39 (dd, J = 8.5, 7.7 Hz, 1H), 4.80 (s, 3H), 4.00 (q, J = 7.1 Hz, 4H), 1.30 (t, J = 7.1 Hz, 6H). ^{13}C NMR (100 MHz, CD_3OD) δ_C (ppm) 145.73, 142.53, 136.62, 135.73, 130.64, 130.41, 125.44, 125.35, 123.26, 122.90, 120.89, 119.68, 115.68, 113.10, 111.49, 45.78, 36.73, 11.27.

N^1,N^1-Dimethylpropane-1,2-diamine (12). To a solution of NH_4OAc (5.26 g, 68.2 mmol), $NaBH_3CN$ (0.634 g, 10 mmol), and anhydrous $MgSO_4$ (8 g) in dry MeOH was added 1-(dimethylamino)propan-2-one **11** (0.863 g, 8.5 mmol, 1 mL). The reaction mixture was refluxed for 20 h. After this period, the $MgSO_4$ was removed and the reaction mixture acidified with concentrated HCl to pH 2. The solvent was removed at reduced pressure and the crude product dissolved in water (50 mL). The aqueous solution was washed with Et_2O (3 × 20 mL), treated with NaOH 10% to pH 10, and extracted with CH_2Cl_2 (3 × 20 mL). The organic extracts were washed with water and brine, dried (anhydrous Na_2SO_4), and the solvent removed under reduced pressure to give **12**, 24% (204.2 mg), as a light-brown oil. ^{1}H NMR (400 MHz, $CDCl_3$) δ_H (ppm) 3.00 (m, 1H), 2.18 (s, 6H), 2.12 (d, J = 10.1 Hz, 1H), 2.04 (dd, J = 4.2, 4.1 Hz, 1H), 1.01 (d, J = 6.89 Hz, 3H). ^{13}C NMR (100 MHz, $CDCl_3$) δ_C (ppm) 68.20, 45.82, 44.14, 21.07.

2-(3-(Piperidin-1-yl)-propyl)isoindoline-1,3-dione (14). To a solution of *N*-(3-bromopropyl)phthalimide **13** (2.71 g, 10.1 mmol) and TEA (1.67 mL, 24.2 mmol) in CH_2Cl_2 (40 mL) was added piperidine (1 mL, 10.1 mmol). The reaction mixture was refluxed 30 h, and after this period, the solvent was removed under reduced pressure. The crude residue was purified by column chromatography (CH_2Cl_2 and CH_2Cl_2:MeOH (9:1)) to afford **14**, 1.45 g (51%) as a white solid, mp 266−267 °C. ^{1}H NMR (400 MHz, $CDCl_3$) δ_H (ppm) 7.83 (dd, J = 5.2, 3.1 Hz, 2H), 7.73 (dd, J = 5.2, 3.1 Hz, 2H), 3.78 (t, J = 6.57 Hz, 2H), 3.06−2.66 (m, 6H), 2.23 (quintet, J = 7.2 Hz, 2H), 1.90 (m, 4H), 1.57 (m, 2H). ^{13}C NMR (100 MHz, $CDCl_3$) δ_C (ppm) 168.18, 134.08, 131.81, 123.28, 55.63, 53.64, 35.66, 23.93, 23.38, 22.58.

3-Piperidin-1-yl-propan-1-amine (15). To a solution of **14** (0.5 g, 1.83 mmol) in EtOH (30 mL) was added hydrazine (0.552 mL, 4.38 mmol). The reaction mixture was refluxed 3 h, and the resulting precipitate was collected and the solvent removed under reduced pressure. The crude product was dissolved in CH_2Cl_2, the precipitate was again collected and the solvent evaporated under reduced pressure to give **15**, 71% yield (178 mg) as a light-brown oil. ^{1}H NMR (400 MHz, $CDCl_3$) δ_H (ppm) 2.98 (s, 1H), 2.75 (t, J = 6.3 Hz, 2H), 2.39 (m, 6H), 1.63 (quintet, J = 6.9 Hz, 2H), 1.54 (m, 4H), 1.38 (m, 2H). ^{13}C NMR (100 MHz, $CDCl_3$) δ_C (ppm) 57.19, 54.34, 40.69, 28.86, 25.62, 24.07.

***tert*-Butyl 4-(diethylamino)butylcarbamate (17).** A mixture of *tert*-butyl 4-aminobutylcarbamate **16** (0.1 mL, 0.52 mmol), anhydrous $MgSO_4$ (2 g), and $NaBH_3CN$ (70.4 mg, 1.25 mmol) in dry MeOH (5 mL) was cooled to 0 °C. Acetaldehyde (1 mL) was added and reaction allowed to continue for 2 h in an ice bath. After this period, the anhydrous $MgSO_4$ was collected by filtration and the solvent removed under reduced pressure. The crude product was dissolved in water (5 mL), basified to pH 10 with aqueous KOH 5%, and extracted with CH_2Cl_2 (3 × 20 mL). The combined organic extracts were washed with water and brine, dried (anhydrous Na_2SO_4), and evaporated under reduced pressure to give **17**, in 94% yield (119.9 mg) as yellow oil. ^{1}H NMR (400 MHz, $CDCl_3$) δ_H (ppm) 5.42 (s, NH), 2.95 (d, J = 5.3 Hz, 2H), 2.43 (q, J = 7.1 Hz, 4H), 2.32 (t, J = 6.5 Hz, 2H), 1.36 (s broad, 4H), 1.27 (s, 9H), 0.90 (t, J = 7.1 Hz, 6H). ^{13}C NMR (100 MHz, $CDCl_3$) δ_C (ppm) 155.77, 78.21, 51.96, 46.09, 39.89, 27.99, 27.65, 23.55, 10.55.

N^1,N^1-Diethylbutane-1,4-diamine (18). A solution of **17** (119.9 mg, 0.49 mmol) in CH_2Cl_2:TFA (1:1, 2 mL) was stirred at room temperature for 1 h. Solvent was removed under reduced pressure, and the crude residue neutralized with aqueous KOH (2 M). The aqueous solution was then extracted with CH_2Cl_2 (3 × 10 mL). The combined organic extracts were washed with water and brine, dried (anhydrous Na_2SO_4), and evaporated under reduced pressure to give **18**, 63% yield (44.8 mg), as a yellow oil. ^{1}H NMR (400 MHz, $CDCl_3$) δ_H (ppm) 4.02 (s, NH_2), 2.70 (t, J = 6.2 Hz, 2H), 2.50 (q, J = 7.1 Hz, 4H), 2.39 (t, J = 6.7 Hz, 2H), 1.50 (m, 4H), 0.97 (t, J = 7.1 Hz, 6H). ^{13}C NMR (100 MHz, $CDCl_3$) δ_C (ppm) 52.14, 45.98, 40.92, 30.01, 24.12, 10.60.

***N*-{4-[(Diethylamino)methyl]-3-hydroxyphenyl}acetamide (20).** To a solution of *N*-(3-hydroxyphenyl)acetamide **19** (2 g, 13.2 mmol) and formaldehyde (0.73 mL, 26.4 mmol) in EtOH (20 mL) was added diethylamine (2.74 mL, 26.4 mmol). The mixture was refluxed for 96 h, and after this period, the solvent

was removed under reduced pressure. The remaining residue was dissolved in CH_2Cl_2 (20 mL) and extracted with HCl 0.1 M (4 × 50 mL). The combined aqueous extracts were basified to pH 10 with KOH 5% and extracted with CH_2Cl_2 (3 × 20 mL). The organic extracts were washed with H_2O and dried with NaCl (satd) and anhydrous Na_2SO_4. Evaporation of the solvent gave **20** as yellow oil, in 55% yield. ^{1}H NMR (400 MHz, $CDCl_3$) δ_H (ppm) 8.08 (s, OH), 7.05 (d, J = 7.9 Hz, 1H), 6.90 (s, 1H), 6.88 (d, J = 7.9 Hz, 1H), 3.71 (s, 2H), 2.60 (q, J = 6.7 Hz, 4H), 2.11 (s, 3H), 1.08 (t, J = 6.7 Hz, 6H). ^{13}C NMR (100 MHz, $CDCl_3$) δ_C ppm 168.46, 158.08, 138.12, 128.25, 117.41, 110.34, 107.19, 55.86, 45.70, 24.01, 10.63.

In Vitro Cytotoxicity. Vero cells (monkey kidney epithelium) were kindly donated by the Departamento de Virología, Facultad de Microbiología, Universidad de Costa Rica. Cells were maintained in Dulbecco essential medium supplemented with 10% fetal bovine serum, 2 mmol/L of glutamine, 100 IU/mL of penicillin, and amphotericin B in a 37 °C humidified incubator under an atmosphere of 7% CO_2 on air. For the experiments, cells were cultured in 96-well plates (15000 cells/well) and allowed to adhere overnight. Sample stocks were prepared in DMSO at a concentration of 30 mg/mL. Log dilutions made on culture medium were tested on cells for 48 h. Doxorubicin hydrochloride (Sigma-Aldrich) was used as a standard for the experiments.

After cells were treated with the compounds, MTT [3-(4,5-dimethylthiazol-2-yl)-2,5-diphenyltetrazolium bromide] reagent (final concentration of 0.5 mg/mL) was added to the culture medium and, after incubation for 2 h at 37 °C, it was carefully removed and 95% ethanol was added to the wells to dissolve formazan crystals.[56] Absorbances were read at 570 nm, and results were calculated as viability percentages, using samples incubated with DMSO dissolved in culture medium as 100% viability values. IC_{50} values were obtained from a concentration vs viability curve using SlideWrite Plus 6.1 (Advanced Graphics Software, Inc., Carlsbad, CA).

In Vitro Antiplasmodial Activity in Human Red Blood Cells. Human red blood cells infected with 1% ring stage *P. falciparum* strains synchronized with 5% sorbitol were incubated with tested compounds in 96-well plates at 37 °C for 48 h in RPMI-1640 medium, supplemented with 25 mM HEPES pH 7.4, 10% heat inactivated human serum (or 0.5% Albumax, 2% human serum), and 100 μM hypoxanthine under an atmosphere of 3% O_2, 5% CO_2, 91% N_2. After 48 h, the cells were fixed in 2% formaldehyde in PBS, transferred into PBS with 100 mM NH_4Cl, 0.1% Triton X-100, 1 nM YOYO-1, and then analyzed in a flow cytometer (FACSort, Beckton Dickinson; EX 488 nm, EM 520 nm.) Values of IC_{50} were calculated using GraphPad PRISM software.

In Vitro Antiplasmodial Activity in Human Hepatoma Cells. In vitro infection of Huh7 cells, a human hepatoma cell line, was determined by analyzing cells infected with GFP-expressing *P. berghei* parasites by fluorescence-activated cell sorting (FACS), as described previously.[37] Cell samples for FACS analysis were washed with 1 mL of phosphate buffered saline (PBS), incubated with 100 μL of trypsin for 5 min at 37 °C, and collected in 400 μL of 10% v/v FCS in PBS at the selected time points post sporozoite addition. Cells were then centrifuged at 0.1*g* for 5 min at 4 °C and resuspended in 150 μL of 2% v/v FCS in PBS. Cells were analyzed on a Becton Dickinson FACScalibur with the appropriate settings for the fluorophore used. Data acquisition and analysis were carried out using the CELLQuest (version 3.2.1fl1, Becton Dickinson) and FlowJo (version 6.3.4, FlowJo) software packages, respectively. Invasion was assessed by determining the percentage of GFP-positive cells 2 h after sporozoite addition; intracellular parasite development was assessed by measuring the fluorescence intensity of GFP-positive cells 48 h after addition of the parasites to the cells.

Binding to d(GATCCTAGGATC)$_2$. Titrations were carried out using spectrophotofluorimetry or UV−visible spectrophotometry in 1 cm quartz cuvettes by adding aliquots of a stock solution (0.027 or 0.27 mM) of 12-mer oligonucleotide duplex to a solution (0.5, 1, or 5 μM) of the ligand in 0.01 M phosphate buffer (pH 7.4) containing 0.1 M NaCl. All the spectrophotofluorimetric titration spectra were recorded at an excitation wavelength of 339 nm and an emission wavelength between 450 and 500 nm. Dissociation constants of cryptolepine analogues in complex with the 12-mer DNA oligonucleotide d(GATCCTAGGATC)$_2$ were determined by fitting the experimental data to the single binding site model (eq 1) using least-squares nonlinear regression analysis. For some compounds, the required equation was that for two binding sites sequestering ligand independently of each other and with relatively weak binding in the second binding equilibrium detectable at higher values of [DNA]. The general equation for the two-site binding model is

$$F = \{F_{max}[DNA]/(K_d + [DNA])\} + \{F'_{max}[DNA]/(K'_d + [DNA])\} \quad (4)$$

where F'_{max} and K'_d are the binding parameters for the second equilibrium. If $K'_d \gg$ [DNA], this reduces to eq 3. Data were fit to the equations supplied with GraphPad PRISM computer program (GraphPad software, version 5.00, San Diego, CA) or to appropriate variants written into that program. Best models were decided by χ-squared parameters and the distribution of the residuals. Association constants were calculated from dissociation constants.

Heme Binding Studies. Titrations of FPIX-OH in buffered 40% DMSO (v/v) at pH 5.5, with chloroquine, cryptolepine, and analogues, were made according to the following procedure. Stock solutions of hematin and ligands were obtained by dissolving compounds in UV-spectroscopy grade DMSO to a concentration of 1 mM, with storage in the dark. Aqueous buffered DMSO (40% v/v, 1 mL) solutions of hematin, chloroquine, cryptolepine, and analogues were prepared daily from stock solution (100 μM). Hematin solutions (10 μM) were prepared with buffered 40% DMSO (v/v) solution and transferred to cuvettes. Solutions of chloroquine, cryptolepine, and analogues (100 μM) were initially added to the cuvette in amounts as small as 2 μL (gradually increasing the volume in subsequent additions) until final concentrations higher than the hematin concentration were achieved. After each addition, the cuvette was stirred for 1 min before the absorbance was read. UV−visible titrations were performed between 230 and 500 nm to incorporate the Soret band of porphyrin. The UV−visible spectrum obtained after each titrated addition was analyzed and stacked against the corresponding absorbances. Dissociation constants of chloroquine, cryptolepine, and analogues complexed with FPIX-OH were determined by fitting the experimental data to the appropriate equation models[49,52] using least-squares nonlinear regression analysis with GraphPad PRISM software. Models were analyzed by χ-squared parameters. Association constants, K_{ass}, were calculated from dissociation constants.

Binding Stoichiometries. Binding stoichiometries for cryptolepine analogues:12-mer ds-DNA complexes were monitored by spectrophotofluorimetry or UV−visible spectrophotometry using the Job method of continuous variation.[41,57] The total concentration of DNA and cryptolepine ligand in the solutions was kept constant, and the changes in fluorescence or absorbance intensity monitored as a function of the mole fraction of cryptolepine ligand. The intercept of the two best-fit lines obtained by least-squares linear regression analysis indicated the binding stoichiometry of the complex.

Binding stoichiometries for chloroquine, cryptolepine, and analogues with FPIX-OH were monitored by UV−visible spectrophotometry using the Job method of continuous variation[41,57] in buffered 40% v/v DMSO (pH 5.5). Buffered 40% DMSO solution was prepared in a 250 mL volume using DMSO (100 mL), aqueous HEPES (1M, 5 mL), and deionized water. The sum of the concentrations of the ligand and FPIX-OH was kept constant

([ligand] + [FPIX-OH] = 10 μM). The absorbance changes of the Soret band was measured at 402 nm. In Figure 7, y is the corrected absorbance ($y = -\{A - (\varepsilon_{\text{FPIX-OH}}[\text{FPIX-OH}] + \varepsilon_{\text{compound}}[\text{compound}])b\}$), where A is the measured absorbance, $\varepsilon_{\text{FPIX-OH}}$ and $\varepsilon_{\text{compound}}$ are the molar absorptivities of hematin and ligands, respectively, and b the optical path length.[58] The intercept of the two best-fit lines obtained by least-squares linear regression analysis indicated the binding stoichiometry of the complex.

Compound Localization in *P. falciparum*-Infected Erythrocytes. *P. falciparum* blood stages were cultured in human erythrocytes as previously described.[59] Intracellular localization of compounds **1** and **3n** was performed by fluorescence microscopy on a Zeiss Axiovert 200 M microscope equipped with an oil-immersion 100× Plan-apochromat 1.4NA objective. A human red blood cell culture with 1.9% parasitemia was incubated with 5 μM of each of the compounds or with an equivalent amount of the DMSO solvent (control) for 3 h, at room temperature, in the dark, and observed on poly-Lys-coated coverslips after gentle washing with PBS to remove nonadherent cells. Fluorescence intensity quantification and plot profiles were made with ImageJ software.

Acknowledgment. This work was supported by Fundação para a Ciência e Tecnologia (project PTDC/SAU-FAR/114864/2009), British Council (B-4/07), FEES-Vicerrectoría de Investigación, Universidad de Costa Rica (project 809-A8-518), and CYTED network RIBIOFAR (RT-0282). J.L. thanks FCT for a Ph.D. grant (SFRH/BD/29202/2006). M.P. was hired under the Ciência program of the Portuguese Ministry of Science and Technology. We acknowledge Rosângela Frita for the *P. falciparum*-infected human blood culture.

Supporting Information Available: NMR spectra of cryptolepine derivatives **3a**−**y**, elemental analysis (C, H, N), high resolution mass spectrometry, data from equilibrium binding studies with FPIX-OH (determination of stoichiometry, association constants of complexes, and fluorescence quenching) and DNA (determination of stoichiometry and association constants of complexes) of cryptolepine and analogues, as well as geometry optimization images of some cryptolepine analogues, at an ab initio quantum mechanics level by using density functional theory (DFT). This material is available free of charge via the Internet at http://pubs.acs.org.

References

(1) Martinelli, A.; Moreira, R.; Cravo, P. V. L. Malaria combination therapies: advantages and shortcomings. *Mini Rev. Med. Chem.* **2008**, *8*, 201–212.
(2) Fidock, D. A.; Eastman, R. T.; Ward, S. A.; Meshnick, S. R. Recent highlights in antimalarial drug resistance and chemotherapy research. *Trends Parasitol.* **2008**, *24*, 537–544.
(3) Ridley, R. G. Medical need, scientific opportunity and the drive for antimalarial drugs. *Nature* **2002**, *415*, 686–693.
(4) Kaur, K.; Jain, M.; Kaur, T.; Jain, R. Antimalarials from nature. *Bioorg. Med. Chem.* **2009**, *17*, 3229–3256.
(5) Kumar, V.; Mahajan, A.; Chibale, K. Synthetic medicinal chemistry of selected antimalarial natural products. *Bioorg. Med. Chem.* **2009**, *17*, 2236–2275.
(6) Krettli, A. U.; Adebayo, J. O.; Krettli, L. G. Testing of Natural Products and Synthetic Molecules Aiming at New Antimalarials. *Curr. Drug Targets* **2009**, *10*, 261–270.
(7) van Agtmael, M. A.; Eggelte, T. A.; van Boxtel, C. J. Artemisinin drugs in the treatment of malaria: from medicinal herb to registered medication. *Trends Pharmacol. Sci.* **1999**, *20*, 199–205.
(8) Bray, P. G.; Ward, S. A.; O'Neill, P. M. Quinolines and artemisinin: chemistry, biology and history. *Malar.: Drugs Dis. Post-Genom. Biol.* **2005**, *295*, 3–38.
(9) Clinquart, E. Sur la Compesition Chimnique de *Cryptolepis triangularis* plante congolaise. *Bull. Acad. R. Med. Belg.* **1929**, *12*, 627–635.
(10) Kumar, E.; Etukala, J. R.; Ablordeppey, S. Y. Indolo[3,2-*b*]-quinolines: synthesis, biological evaluation and structure−activity relationships. *Mini Rev. Med. Chem.* **2008**, *8*, 538–554.
(11) Wright, C. W. Recent developments in naturally derived antimalarials: cryptolepine analogues. *J. Pharm. Pharmacol.* **2007**, *59*, 899–904.
(12) Lisgarten, J. N.; Coll, M.; Portugal, J.; Wright, C. W.; Aymami, J. The antimalarial and cytotoxic drug cryptolepine intercalates into DNA at cytosine−cytosine sites. *Nature Struct. Biol.* **2002**, *9*, 57–60.
(13) Dassonneville, L.; Bonjean, K.; De Pauw-Gillet, M. C.; Colson, P.; Houssier, C.; Quetin-Leclercq, J.; Angenot, L.; Bailly, C. Stimulation of topoisomerase II-mediated DNA cleavage by three DNA-intercalating plant alkaloids: cryptolepine, matadine, and serpentine. *Biochemistry* **1999**, *38*, 7719–7726.
(14) Ansah, C.; Gooderham, N. J. The Popular Herbal Antimalarial, Extract of *Cryptolepis sanguinolenta*, Is Potently Cytotoxic. *Toxicol. Sci.* **2002**, *70*, 245–251.
(15) Paulo, A.; Gomes, E. T.; Steele, J.; Warhurst, D. C.; Houghton, P. J. Antiplasmodial activity of *Cryptolepis sanguinolenta* alkaloids from leaves and roots. *Planta Med.* **2000**, *66*, 30–34.
(16) Ansah, C.; Khan, A.; Gooderham, N. J. In vitro genotoxicity of the West African anti-malarial herbal *Cryptolepis sanguinolenta* and its major alkaloid cryptolepine. *Toxicology* **2005**, *208*, 141–147.
(17) Bray, P. G.; Mungthin, M.; Ridley, R. G.; Ward, S. A. Access to hematin: the basis of chloroquine resistance. *Mol. Pharmacol.* **1998**, *54*, 170–179.
(18) O'Neill, P. M.; Bray, P. G.; Hawley, S. R.; Ward, S. A.; Park, B. K. 4-aminoquinolines—past, present, and future: a chemical perspective. *Pharmacol. Ther.* **1998**, *77*, 29–58.
(19) Hawley, S. R.; Bray, P. G.; Mungthin, M.; Atkinson, J. D.; O'Neill, P. M.; Ward, S. A. Relationship between antimalarial drug activity, accumulation, and inhibition of heme polymerization in *Plasmodium falciparum* in vitro. *Antimicrob. Agents Chemother.* **1998**, *42*, 682–686.
(20) Wright, C. W.; Addae-Kyereme, J.; Breen, A. G.; Brown, J. E.; Cox, M. F.; Croft, S. L.; Gokcek, Y.; Kendrick, H.; Phillips, R. M.; Pollet, P. L. Synthesis and evaluation of cryptolepine analogues for their potential as new antimalarial agents. *J. Med. Chem.* **2001**, *44*, 3187–3194.
(21) Weissbuch, I.; Leiserowitz, L. Interplay Between Malaria, Crystalline Hemozoin Formation, and Antimalarial Drug Action and Design. *Chem. Rev.* **2008**, *108*, 4899–4914.
(22) Buller, R.; Peterson, M. L.; Almarsson, O.; Leiserowitz, L. Quinoline binding site on malaria pigment crystal: a rational pathway for antimalarial drug design. *Cryst. Growth Des.* **2002**, *2*, 553–562.
(23) Arzel, E.; Rocca, P.; Grellier, P.; Labaeid, M.; Frappier, F.; Gueritte, F.; Gaspard, C.; Marsais, F.; Godard, A.; Queguiner, G. New synthesis of benzo-delta-carbolines, cryptolepines, and their salts: in vitro cytotoxic, antiplasmodial, and antitrypanosomal activities of delta-caribolines, benzo-delta-carbolines, and cryptolepines. *J. Med. Chem.* **2001**, *44*, 949–960.
(24) Lavrado, J.; Paulo, A.; Gut, J.; Rosenthal, P. J.; Moreira, R. Cryptolepine analogues containing basic aminoalkyl side-chains at C-11: synthesis, antiplasmodial activity, and cytotoxicity. *Bioorg. Med. Chem. Lett.* **2008**, *18*, 1378–81.
(25) Gorlitzer, K.; Weber, J. Fused Quinolines 5. 10-Hydroxy-10*H*-Indolo[3,2-*b*]Quinoline 5-Oxide (Dioxyquindoline). *Arch. Pharm. (Weinheim, Ger.)* **1981**, *314*, 850–852.
(26) Gorlitzer, K.; Weber, J. Fused Quinolines 6. 10*H*-Indolo[3,2-*b*]-Quinolines. *Arch. Pharm. (Weinheim, Ger.)* **1981**, *314*, 852–861.
(27) Bierer, D. E.; Dubenko, L. G.; Zhang, P. S.; Lu, Q.; Imbach, P. A.; Garofalo, A. W.; Phuan, P. W.; Fort, D. M.; Litvak, J.; Gerber, R. E.; Sloan, B.; Luo, J.; Cooper, R.; Reaven, G. M. Antihyperglycemic activities of cryptolepine analogues: an ethnobotanical lead structure isolated from *Cryptolepis sanguinolenta*. *J. Med. Chem.* **1998**, *41*, 2754–2764.
(28) Bierer, D. E.; Fort, D. M.; Mendez, C. D.; Luo, J.; Imbach, P. A.; Dubenko, L. G.; Jolad, S. D.; Gerber, R. E.; Litvak, J.; Lu, Q.; Zhang, P. S.; Reed, M. J.; Waldeck, N.; Bruening, R. C.; Noamesi, B. K.; Hector, R. F.; Carlson, T. J.; King, S. R. Ethnobotanical-directed discovery of the antihyperglycemic properties of cryptolepine: its isolation from *Cryptolepis sanguinolenta*, synthesis, and in vitro and in vivo activities. *J. Med. Chem.* **1998**, *41*, 894–901.
(29) Ridley, R. G.; Hofheinz, W.; Matile, H.; Jaquet, C.; Dorn, A.; Masciadri, R.; Jolidon, S.; Richter, W. F.; Guenzi, A.; Girometta, M. A.; Urwyler, H.; Huber, W.; Thaithong, S.; Peters, W. 4-Aminoquinoline analogs of chloroquine with shortened side chains retain activity against chloroquine-resistant *Plasmodium falciparum*. *Antimicrob. Agents Chemother.* **1996**, *40*, 1846–1854.
(30) De, D. Y. D.; Krogstad, F. M.; Byers, L. D.; Krogstad, D. J. Structure−activity relationships for antiplasmodial activity among 7-substituted 4-aminoquinolines. *J. Med. Chem.* **1998**, *41*, 4918–4926.
(31) Madrid, P. B.; Sherrill, J.; Liou, A. P.; Weisman, J. L.; DeRisi, J. L.; Guy, R. K. Synthesis of ring-substituted 4-aminoquinolines and

evaluation of their antimalarial activities. *Bioorg. Med. Chem. Lett.* **2005**, *15*, 1015–1018.
(32) O'Neill, P. M.; Mukhtar, A.; Stocks, P. A.; Randle, L. E.; Hindley, S.; Ward, S. A.; Storr, R. C.; Bickley, J. F.; O'Neil, I. A.; Maggs, J. L.; Hughes, R. H.; Winstanley, P. A.; Bray, P. G.; Park, B. K. Isoquine and related amodiaquine analogues: a new generation of improved 4-aminoquinoline antimalarials. *J. Med. Chem.* **2003**, *46*, 4933–4945.
(33) O'Neill, P. M.; Ward, S. A.; Berry, N. G.; Jeyadevan, J. P.; Biagini, G. A.; Asadollaly, E.; Park, B. K.; Bray, P. G. A medicinal chemistry perspective on 4-aminoquinoline antimalarial drugs. *Curr. Top. Med. Chem* **2006**, *6*, 479–507.
(34) O'Neill, P. M.; Park, B. K.; Shone, A. E.; Maggs, J. L.; Roberts, P.; Stocks, P. A.; Biagini, G. A.; Bray, P. G.; Gibbons, P.; Berry, N.; Winstanley, P. A.; Mukhtar, A.; Bonar-Law, R.; Hindley, S.; Bambal, R. B.; Davis, C. B.; Bates, M.; Hart, T. K.; Gresham, S. L.; Lawrence, R. M.; Brigandi, R. A.; Gomez-Delas-Heras, F. M.; Gargallo, D. V.; Ward, S. A. Candidate Selection and Preclinical Evaluation of *N-tert*-Butyl Isoquine (GSK369796), An Affordable and Effective 4-Aminoquinoline Antimalarial for the 21st Century. *J. Med. Chem.* **2009**, *52*, 1408–1415.
(35) Madrid, P. B.; Liou, A. P.; DeRisi, J. L.; Guy, R. K. Incorporation of an intramolecular hydrogen-bonding motif in the side chain of 4-aminoquinolines enhances activity against drug-resistant *P. falciparum*. *J. Med. Chem.* **2006**, *49*, 4535–4543.
(36) Onyeibor, O.; Croft, S. L.; Dodson, H. I.; Feiz-Haddad, M.; Kendrick, H.; Millington, N. J.; Parapini, S.; Phillips, R. M.; Seville, S.; Shnyder, S. D.; Taramelli, D.; Wright, C. W. Synthesis of some cryptolepine analogues, assessment of their antimalarial and cytotoxic activities, and consideration of their antimalarial mode of action. *J. Med. Chem.* **2005**, *48*, 2701–2709.
(37) Prudencio, M.; Rodrigues, C. D.; Ataide, R.; Mota, M. M. Dissecting in vitro host cell infection by *Plasmodium* sporozoites using flow cytometry. *Cell. Microbiol.* **2008**, *10*, 218–224.
(38) Stocks, P. A.; Bray, P. G.; Barton, V. E.; Al-Helal, M.; Jones, M.; Araujo, N. C.; Gibbons, P.; Ward, S. A.; Hughes, R. H.; BiaginiG. A.; Davies, J.; Amewu, R.; Mercer, A. E.; Ellis, G.; O'Neill, P. M. Evidence for a common non-heme chelatable-iron-dependent activation mechanism for semisynthetic and synthetic endoperoxide antimalarial drugs. *Angew. Chem., Int. Ed.* **2007**, *46*, 6278–6283.
(39) Wenzel, N. I.; Chavain, N.; Wang, Y. L.; Friebolin, W.; Maes, L.; Pradines, B.; Lanzer, M.; Yardley, V.; Brun, R.; Herold-Mende, C.; Biot, C.; Toth, K.; Davioud-Charvet, E. Antimalarial versus Cytotoxic Properties of Dual Drugs Derived From 4-Aminoquinolines and Mannich Bases: Interaction with DNA. *J. Med. Chem.* **2010**, *53*, 3214–3226.
(40) Bonjean, K.; De Pauw-Gillet, M. C.; Defresne, M. P.; Colson, P.; Houssier, C.; Dassonneville, L.; Bailly, C.; Greimers, R.; Wright, C.; Quetin-Leclercq, J.; Tits, M.; Angenot, L. The DNA intercalating alkaloid cryptolepine interferes with topoisomerase II and inhibits primarily DNA synthesis in B16 melanoma cells. *Biochemistry* **1998**, *37*, 5136–5146.
(41) Ingham, K. C. Application of Jobs Method of Continuous Variation to Stoichiometry of Protein−Ligand Complexes. *Anal. Biochem.* **1975**, *68*, 660–663.
(42) Huang, C. Y. Determination of Binding Stoichiometry by the Continuous Variation Method—the Job Plot. *Methods Enzymol.* **1982**, *87*, 509–525.
(43) Strickland, J. A.; Marzilli, L. G.; Gay, K. M.; Wilson, W. D. Porphyrin and metalloporphyrin binding to DNA polymers: rate and equilibrium binding studies. *Biochemistry* **1988**, *27*, 8870–8878.
(44) Chirvony, V. S.; Galievsky, V. A.; Terekhov, S. N.; Dzhagarov, B. M.; Ermolenkov, V. V.; Turpin, P. Y. Binding of the Cationic 5-Coordinate Zn(II)-5,10,15,20-tetrakis(4-*N*-methylpyridyl)porphyrin to DNA and Model Polynucleotides: Ionic-Strength Dependent Intercalation in $[Poly(dG\text{-}dC)]_2$. *Biospectroscopy* **1999**, *5*, 302–312.
(45) Pandey, A. V.; Bisht, H.; Babbarwal, V. K.; Srivastava, J.; Pandey, K. C.; Chauhan, V. S. Mechanism of malarial haem detoxification inhibition by chloroquine. *Biochem. J.* **2001**, *355*, 333–338.
(46) Vippagunta, S. R.; Dorn, A.; Ridley, R. G.; Vennerstrom, J. L. Characterization of chloroquine-hematin mu-oxo dimer binding by isothermal titration calorimetry. *Biochim. Biophys. Acta* **2000**, *1475*, 133–140.
(47) O'Neill, P. M.; Shone, A. E.; Stanford, D.; Nixon, G.; Asadollahy, E.; Park, B. K.; Maggs, J. L.; Roberts, P.; Stocks, P. A.; Biagini, G.; Bray, P. G.; Davies, J.; Berry, N.; Hall, C.; Rimmer, K.; Winstanley, P. A.; Hindley, S.; Bambal, R. B.; Davis, C. B.; Bates, M.; Gresham, S. L.; Brigandi, R. A.; Gomez-de-las-Heras, F. M.; Gargallo, D. V.; Parapini, S.; Vivas, L.; Lander, H.; Taramelli, D.; Ward, S. A. Synthesis, Antimalarial Activity, and Preclinical Pharmacology of a Novel Series of 4′-Fluoro and 4′-Chloro Analogues of Amodiaquine. Identification of a Suitable "Back-Up" Compound for *N-tert*-Butyl Isoquine. *J. Med. Chem.* **2009**, *52*, 1828–1844.
(48) Casabianca, L. B.; An, D.; Natarajan, J. K.; Alumasa, J. N.; Roepe, P. D.; Wolf, C.; de Dios, A. C. Quinine and chloroquine differentially perturb heme monomer-dimer equilibrium. *Inorg. Chem.* **2008**, *47*, 6077–6081.
(49) Egan, T. J.; Mavuso, W. W.; Ross, D. C.; Marques, H. M. Thermodynamic factors controlling the interaction of quinoline antimalarial drugs with ferriprotoporphyrin IX. *J. Inorg. Biochem.* **1997**, *68*, 137–145.
(50) Egan, T. J.; Ncokazi, K. K. Effects of solvent composition and ionic strength on the interaction of quinoline antimalarials with ferriprotoporphyrin IX. *J. Inorg. Biochem.* **2004**, *98*, 144–152.
(51) Marques, H. M.; Munro, O. Q.; Crawcour, M. L. Coordination of N-Donor Ligands by Hematohemin. *Inorg. Chim. Acta* **1992**, *196*, 221–229.
(52) Kelly, J. X.; Winter, R.; Peyton, D. H.; Hinrichs, D. J.; Riscoe, M. Optimization of xanthones for antimalarial activity: the 3,6-bis-omega-diethylaminoalkoxyxanthone series. *Antimicrob. Agents Chemother.* **2002**, *46*, 144–150.
(53) Sajid, M.; McKerrow, J. H. Cysteine proteases of parasitic organisms. *Mol. Biochem. Parasitol.* **2002**, *120*, 1–21.
(54) Dahl, E. L.; Rosenthal, P. J. Biosynthesis, localization, and processing of falcipain cysteine proteases of *Plasmodium falciparum*. *Mol. Biochem. Parasitol.* **2005**, *139*, 205–212.
(55) Olson, J. E.; Lee, G. K.; Semenov, A.; Rosenthal, P. J. Antimalarial effects in mice of orally administered peptidyl cysteine protease inhibitors. *Bioorg. Med. Chem.* **1999**, *7*, 633–638.
(56) Denizot, F.; Lang, R. Rapid Colorimetric Assay for Cell-Growth and Survival—Modifications to the Tetrazolium Dye Procedure Giving Improved Sensitivity and Reliability. *J. Immunol. Methods* **1986**, *89*, 271–277.
(57) Job, P. Studies on the formation of complex minerals in solution and on their stability. *Ann. Chim.* (*Cachan, Fr.*) **1928**, *9*, 113–203.
(58) Hill, Z. D.; Maccarthy, P. Novel Approach to Job Method—an Undergraduate Experiment. *J. Chem. Educ.* **1986**, *63*, 162–167.
(59) Moll, K.; Ljungström, I.; Perlmann, H.; Scherf, A.; Wahlgren, M. *Methods in Malaria Research*; Malaria Research and Reference Reagent Resource Center: Manassas, VA, 2008; p 330.